A Probabilistic Landslide Risk Assessment (LRA) on NH31A and Settlement in Rorachu Watershed, East Sikkim, India by using Bivariate Models and Geospatial Techniques

Sk Asraful Alam (alamrsgis13@gmail.com)
Vidyasagar University https://orcid.org/0000-0002-9501-9198
Sujit Mandal
Diamond Harbour Women's University
Ramkrishna Maity
Vidyasagar University

Research Article

Keywords: Landslide Susceptibility Zone (LSZ), Landslide Risk Assessment (LRA), Success Rate Curve (SRC), Receive Operating Characteristics (ROC), Landslide density (LD).

Posted Date: November 16th, 2021

DOI: https://doi.org/10.21203/rs.3.rs-1019380/v1

A Probabilistic Landslide Risk Assessment (LRA) on NH31A and Settlement in Rorachu Watershed, East Sikkim, India by using Bivariate Models and Geospatial Techniques

Sk Asraful Alam[1*], Sujit Mandal[2], Ramkrishna Maity[1]

[1*]Sk Asraful Alam
Research Scholar
Department of Earth System Science (ESS)
Vidyasagar University, Midnapore
Gmail – alamrsgis13@gmail.com

[2]Sujit Mandal
Professor and Head, Dept. of Geography,
Diamond Harbour Women's University, Sarisha
Gmail - mandalsujit2009@gmail.com

[1]Ramkrishna Maity
Professor and Head, Dept. of Geography & Environment Management
Vidyasagar University, Midnapore
Gmail - ramkrishna@mail.vidyasagar.ac.in

* Corresponding Author
Gmail address: alamrsgis13@gmail.com (Sk Asraful Alam)

Abstract

The Sikkim Himalaya has been recognized as region enormously susceptible slope instability. The NH 31A road falls with east Sikkim Himalaya which has highly deformed by numerous landslide events. Over the few years the NH 31A road sections and settlement with its surrounding areas are invaded by landslide events. To resolve the problem connected to landslide, landslide susceptibility zones (LSZ) and landslide risk assessment (LRA) is an urgent and safe mitigation measure to helping the strategic planning for local people. The present study is an endeavor to take advantage of bivariate statistical method called frequency ratio (FR), information value (IV) and certainty factor (CF) analysis for LSZ and LRA map and attempt to get out the triggering factors for the LSI and LRA in Rorachu watershed, East Sikkim. The landslide inventory map was made by the more premature reports, aerial photograph, Google Earth image and multiple field visits. A total 153 landslides location were mapped using GIS software and divided into 70 % (107) for training data for the modeling using FR, IV and CF models and remaining 30 % (46) were used for validating the models. The thirteen landslide causative factors Geology, Soil, Elevations, Slope, Curvature, drainage Density (DD), Road Density (RD), Rainfall, Normalize Difference Vegetation Index (NDVI), Land Use Land Cover (LULC), Topographic Position Index (TPI), Stream Power Index (SPI) and Topographic Wetness Index (TWI) were extracted from spatial database for the LSZ mapping using FR, IV and CF models. The landslide susceptibility zonation (LSM) map also tested by the histogram and density plot, this is elicited most of the triggering factors for the landslides in Rorachu watershed. The results have been showing that the slope (35^{o} to 50^{o}), elevations (2,500 – 4,100 m) and rainfall (2000- 2,500 mm and 3,000 – 3,300 mm) is the intensest concentration and density for the landslides. The predictive frequency ratio (FR), information value (IV) and certainty factor (CF) model has been validated by receive operating characteristics (ROC) curve, Success rate curve (SRC) and landslide density (LD) method analysis. The result shows that AUC for success rate curves (SRC) are 0.925 (92.50 %), 0.846 (84.60 %) and 0.868 (86.80 %), respectively for frequency ratio (FR), information value (IV) and certainty factor (CF) models. And the result shows that AUC for prediction rates are 0.828 (82.80 %), 0.750 (75 %) and 0.836 (83.60 %), respectively for the FR, IV and CF models. The element-at-risk (Settlement and Road) is revealed the landslide risk assessment (LRA) have been showing that the most

significant risk of settlements areas by the model of FR (9%), IV (38.59%) and CF (20.90%) and the most significant risk of NH 31A road is FR (20.72%), IV (40.91%) and CF (18.78%). These landslide susceptibility maps and landslide risk assessment (LRA) map can be used for the development of land use planning strategies, saves human loss and important for the planners and mitigation purpose. So remarkable attention should be taken into consideration for the highway construction, deforestation and urbanization.

Key words: Landslide Susceptibility Zone (LSZ), Landslide Risk Assessment (LRA), Success Rate Curve (SRC), Receive Operating Characteristics (ROC), Landslide density (LD),

1. Introduction

Disaster causes by Landslides are one of the most significant geo-environmental disasters of mountain area in the world which has been affected so many human lives around the world and change the evolution of landform. Landslide causes death in the Himalaya approximately more than 200 human live every year (Naithani 1999). According to Centre for Research on the Epidemiology of Disasters (CRED 2009), landslides enumerate for approximately 4.4 % of natural disasters worldwide from 1990 to 2009, with 2.3 % of reported landslides take place in Asia. There are more than 25 % of the mountains in this world where more than 12 % of the people live. Sikkim is one of the Indian states where there are more than 97 % mountains. Massive landslide in Sikkim Himalayas are mainly attributed to frequent rainfall and in many cases associated with deforestation, monsoon rainfalls, soil, geology and human interface. The landslides are increasing trend of vulnerabilities related to unplanned urbanization and agriculture, rapid growth of population, fast paced industrialization, environmental degradation and climate change. For all those reasons, everyone's study landslides which has drawn global attention.

Within last few decades, numerous attempts to landslide susceptibility mapping methods and techniques have been developed by different scientist, geologists, and geomorphologists for the assessment of landslide vulnerability. The landslide susceptibility preparing in three ways, like 1. Deterministic approach 2. Qualitative or heuristic approach and 3. Probabilistic approach. Generally the different landslide susceptibility and hazard mapping given by Varnes (1984),

Carrara et al. (1995), Soeters and van Westen (1996), Aleotti and Chowdhury (1999), Guzzetti et al. (1999) and Wang et al. (2005). Many of these used probabilistic models (Lee and Pradhan 2006; Dahal et al. 2008; Oh et al. 2009; Ozdemir 2009; Yilmaz 2010; Oh and Lee 2011; Demir et al. 2012; Pourghasemi et al. 2012a, b; Mohammady et al. 2012; Xu et al. 2012c). a ditermistic approach envisage slope geometry, characteristics of slope materials and pressure which generated by surface and subsurface water in a physical equation. These approaches are commonly used by (Chowdhury 1976; Chowdhury and Bertoldi 1977; Wu and Sidle 1995; Gokceoglu and Aksoy 1996). This deterministic approach will be applied where ground surface are homogenous, landslides known as simple and surface as well as subsurface hydrological data are available. The approach is not effected where landslide area so complex and complicated. That's why we applied qualitative model for landslide vulnerability assessment zonation. Qualitative methods are subjected to researcher knowledge of understanding susceptibility level and their expertise opinion. Quantitative methods based on numerical expression of the relationship between landslides controlling factors and existing landslide areas in that place. There are different quantitative methods applied by (Zezere, 2002; Saha et al., 2005; Lee and Pradhan, 2007; Lee, Ryu, and Kim, 2007), distribution-free methods (Lee et al., 2007; Choi et al., 2011), deterministic analysis methods (Xie et al., 2004; Zorn and Komac, 2004; Claessens et al., 2006; Tazik et al., 2014). And statistical index model also apply some researcher (Van Westen 1997; Rautela and Lakhera 2000; Cevik and Topal 2003; Tien Bui et al. 2011a; Raman and Punia 2012; Regmi et al. 2013).

Sikkim Himalaya faces frequent landslides per year turn out in thousands of fatalities (Bhasin et al. 2002). In Sikkim, around 36,000 people were killed by landslides (Choubey 1992) in 1968 alone. There are many factors responsible for this slope instability, but the primary controlling factors are slope, rainfall, seismic activity, topographic positioning index (TPI) and anthropogenic activities (Lin et al. 2006; Gupta et al., 2018; Zhang et al., 2018). That's why landslide susceptibility mapping is immensely important for disaster prevention and mitigation, and it will be important for future planning. With the background of the study lots of application landslide vulnerability modeling around the world. We applied three statistical modeling for the landslide vulnerability mapping in Rorochu watershed (Frequency Ratio model, Certainty Factor model and Information value model). Frequency Ratio (FR) has also been applied by (Lee and

Sambath 2006; Lee and Pradhan 2007; Akgun et al. 2008; Yilmaz 2010b; Choi et al. 2012; Ozdemir and Altural 2013; Regmi et al. 2013; Solaimani et al. 2013: Pradhan and Lee 2010a, b). A variety of multivariate approach exist, but those methods commonly used for discremenent analysis and logistic regression (Lee 2007a; Pradhan 2010a). Different other methods have been proposed by different researcher, including Certainty Factor (CF) methods (Binaghi et al., 1998), information values (Wan et al., 2008, Saha et al., 2005;), fuzzy logic (Ercanoglu and Gokceoglu 2002; Kanungo et al. 2006, 2008; Lee 2007b; Muthu et al. 2008; Pradhan and Lee 2009; Pradhan 2010c, c; Pradhan 2011a, b; Pourghasemi et al. 2012c), artificial neural networks (Kanungo et al. 2006; Melchiorre et al. 2008; Chen et al. 2009; Pradhan and Lee 2009, 2010a, b; Pradhan et al. 2010a, b; Pradhan and Buchroithner 2010; Pradhan and Pirasteh 2010; Poudyal et al. 2010; Yilmaz 2009a, b; Yilmaz 2010a, b; Pradhan 2011c; Zare et al. 2012; Bui et al. 2012a),analytical hiarachi process applied by (Ercanoglu et al., 2008; Komac, 2006; Yalcin, 2008; Akgun and Turk, 2010; Mandal and Maiti, 2013).

In this study, although various numerical, statistical, deterministic techniques used for landslide susceptibility and Landslide Risk (LR) analysis have been proposed and implemented. In our study there all data layers of Geology, elevation(DEM), slope, curvature, road density, land use land cover (LULC), NDVI, soil, drainage, drainage density, topographic wetness index and topographic positioning index were taken into account and each class was estimated accordingly with the different mathematical and statistical equation, Combine with the observed landslide inventory was made to perform by FR, CF and IV model process and assess the landslide vulnerability and landslide risk mapping in Rorachu watershed. Frequency Ratio (FR), Certainty Factor (CF) and Information Value (IV) model was successfully applied in this watershed. It is very important to study along this NH31A roads and Settlement landslide vulnerability and landslide risk (LR) assessment mapping because of that there was a national highway which is too much affected by slope instability. The outcomes of the present research will be helpful for the planning and management of this watershed livelihood and national highway.

2. Study area

The study area lies in east Sikkim district which is located in Sikkim Himalaya. It is bounded by the latitudes $27^0$17’14.67” N to $27^0$23’48.50” N and the longitudes $88^0$35’51.40” E to

88043'11.98" E covering an area of around 69.125 km^2 (Fig. 1). High relative reliefs, steep slope along with immensely rugged surfaces are important physiographic characteristics in this state. The maximum and minimum elevation of this Rorachu watershed is 4100 and 816 m respectively. We have said before that there is a very rugged surface here so this Rorachu watershed is no exception. The altitude of this watershed is highly diverse from southwestern periphery (Ranipool) to its northwestern boundary (Pandramaile). The Rorachu watershed feel like tranquil temperature throughout the year with an average maximum temperature 21 ^{0}C during summer session and average minimum temperature 1 ^{0}C during winter session. The slope angle varies from 0^0 to as much as 71^0. The important town of this study area are Gangtok and Tadong whereas Samdong, Ranipool, Deorali are the main small markets. The area is undergoing fast development to urbanization in Gangtok and Ranipool town. Many local roads and highways (NH 31A) going through this watershed areas and new roads will be constructed. The area mostly covers by forest, rocky and barren land, cultivated area and settlements. The physiographic and climatic diversity of this Rorachu watershed and fast developments are increasing the rate of slope instability. That's why we should be analysis the landslide vulnerability modeling for the management practice and future development.

Fig. 1. Location map of the study area

3. Materials and methods

Landslide is one of the most complex movements of the earth. It's very difficult to Identification and mapping of suitable landslide factors for the vulnerability modeling and assessment. The critical point was the selection of accurate pixel size for positional accuracy and precision of the landslide susceptibility levels in the study area (Sahabi et al., 2014). So we must be proper expertise knowledge for the identification of prime factors for the Landslide Susceptibility Index (LSI) and Landslide Risk (LR) modeling. Also, there are no standard guidance for selecting the parameters for slope instability modeling (Ayalew et al., 2005), the nature of the study area, the scale of the analysis, and data availability were taken into account (Yalcin 2008). In this respect, thirteen factors are considering for Landslide susceptibility Index (LSI) and Landslide risk (LR) modeling and analysis (Fig. 2). It is important to compile a digitized database for execution the landslide vulnerability modeling map using GIS. The spatial database has been design and

179 execute for the landslide vulnerability modeling of this study area as shown in (Table 1) In this
180 study, both categorical and continuous data were used for the landslide modeling and ArcGIS
181 10.2, SPSS 23 and R was applied for the entire analysis.

182 Fig. 2. Methodological flow chart

183 Table 1. Sources of data layers of various landslide causative factors

184 ***3.1 Landslide Inventory preparation***

185 Landslide inventory map is that in which it had to be rebuilt by looking at the previous imprint of
186 landslide in this area (Rorachu watershed). In this landslide susceptibility assessment, acquire
187 information about the landslides that have been occurred in the past and this historical
188 information represents the backbone of landslide vulnerability modeling of this study area. This
189 stage envisages as the fundamental part of the landslide vulnerability studies (Guzzetti et al.,
190 1999). Landslide inventory maps serve as a prerequisite for landslide vulnerability modeling
191 study. Accurate detection and identification of landslide is most significant for probabilistic
192 landslide susceptibility analysis. As most of the landslide inventories further verified by (Rawat
193 M.S and Joshi V. 2016; Mondal S. and Mandal K. 2017a). For landslide inventory mapping,
194 address the historical data, detect the remote sensing image and field study were performed. To
195 prepare the Landslide inventory map were performed by the analysis aerial photographs,
196 LANDSAT 8 OLI (30 m) image, Google Earth (Quickbird image, 0.60 m) and GPS survey, at
197 last all the data were vectorized in ArcGIS 10.3 software. In total 153 major and minor
198 landslides were identified in the Rorachu watershed with total area coverage 0.644 sq. km (Fig.
199 3). All the landslides data has been converted vector to raster format for the model preparation.
200 About 107 landslides (70 %) out of the 153 were randomly selected for model training, and
201 remaining 46 (30 %) were used for the model validation purpose. Most of the landslides in this
202 Rorachu watershed area are rock slide, debris slide and earth slide.

203 Fig. 3. Landslide inventory map of Rorachu watershed

204 ***3.2 Selection of landslide conditioning factors***

205 Although enormous studies have been contacted regarding landslide vulnerability analysis been
206 done to develop landside susceptibility map of the Rorachu river basin. There are no such criteria
207 for selecting factors for landslide vulnerability analysis (Ayalew and Yamagishi 2005). The

factors controlling slope instability modeling considered in the present study are including Elevation, Geology, Slope, Soil, Drainage Density (DD), Road Density (RD), Rainfall, Normalize Difference Vegetation Index (NDVI), and Slope curvature, Topographic Position Index (TPI), Stream Power Index (SPI), Topographic Wetness Index (TWI) and Land Use Land Cover (LULC). A particular parameter may be important controlling factors for landslide occurrence in one area but not in another place. All the factors are applied by different researcher in across the globe (Wu et al., 2017).

3.2.1 Geology

It is extensively accepted that geology plays an important role in the occurrence of slope instability because the lithological and structural variations often leads to difference in strength of soil and rocks (Pradhan and Lee 2010a) of this Rorachu watershed. Geologically the study area is characterized by the process of five lithological units including 1.Basic Intrusive, 2. Chungthang Formation, 3.Gorubathan Formation, 4.Lingtse Gnesis, 5.Kanchenjunga Gnesis or Darjeeling Gnesis (undifferentiated) (Fig. 4. Table 2). The geology map of Rorachu watershed was prepared by district resource map of east Sikkim collected from geological survey of india (GSI), Kolkata. Large part of this watershed is covered by Kanchenjunga Gnesis or Darjeeling Gnesis. Lithological unit of basic Kanchenjunga gnesis cover large area (43.02 %) ranked first and followed by Basic intrusive (21.10 %), Chungthang formation (18.48 %), Gorubathan formation (12.12 %) and Lingtse Gnesis (5.35 %). Due to different sets of structural disturbance numerous fractures, faults, cracks and joints are much more probable to slope instability.

Fig. 4. Geology map of the study area

Table 2. Description of geological parameters of Rorachu watershed

3.2.2 Elevation

Elevation or altitude is one of the significant parameter that has been frequently used for landslide conditioning parameters. Altitude control the another parameters of the geographical area. It is controlled by different geological and geomorphological process (Ayalew et al., 2005; Pourghasemi, 2008). In the present study area, the elevation ranges between 816 m to 4100 m (Fig. 5. a). The elevation values were classified into 5 categories with 30 * 30 meter resolution. During the field visit we noticed that most of the landslides are seen in medium and high elevation of the Rorachu watershed area.

3.2.3 Slope

Slope gradient is one of the most significant factors for slope stability assessment (Lee and Min, 2001). Stability of the slope is the interaction between angel of the slope and materials properties of the slope (friction angel, cohesion, porosity, permeability and bonding). Gentle slopes have less probability for slope instability due to lower shear stress (Dai et al., 2001). In contrast, higher the slope gradient higher the shear stresses. In the current study slope map classified five categories using natural breaks method in ArcGIS 10.3. Slope angel ranges from0^0 to 70^o (Fig. 5. b) and there are more than 30 % area under 35^o to 70^o slope angel in this Rorachu watershed.

3.2.4 Soil

Soil is a very important factor for slope instability in mountain area due to soil saturation. Soil saturation becomes significant and affective of any high slope area when it's affective by extensive rainfall. Saturation of soil depends on two factors 1. Intensity, duration and amount of precipitation of this area 2. Soil physical characteristics like, soil texture, structure, porosity, permeability, compactness etc. Soil formation usually takes a long time to develop in mountainous areas that's why soil is not so important for Sikkim Himalaya for landslide vulnerability analysis. Soil develops in very low or gentle slope where geo-environment processes are not so much active. In Rorachu watershed more than 90 % becomes a hilly region. Soil of the Rorachu watershed was divided into six several categories (Fig. 5. c, Table 3) such as 1. Coarse loamy humic dystrudepts, 2. Coarse loamy humic lithic dystrudepts, 3. Coarse loamy typic hapludolls, 4. Fine loamy fluventic eutrudepts, 5. Fine skeletal cumuli hapludolls and 6. Loamy skeletal entic hapludolls. In Rorachu watershed, all soil categories are converted vector polygon to raster format into 30 *30 meter grids.

Table 3. Soil characteristics map of Rorachu watershed (According to Mandal S, Mandal K 2017a)

3.2.5 Drainage Density (DD)

Drainage density is the total length of all streams and rivers of that grid divided by the total area of that grid (Horton, 1932, 1945; Strahler, 1952). Drainage density (DD) indicates the measure of how well or how poorly a river watershed is drained by stream channels. Drainage density

depends on both physical environment and climatic environments of this particular area. Drainage density helps to determine the degree of reducing the shear strength of this slope which has affective for slope instability. In this study, drainage density was assessed by this formula (eq 1)

$$Dd = (Lt/Abasin) \quad (1)$$

Where, D_d represents drainage density, L_T represents total length of the streams in that grid and A_{basin} represent total length of the grid area. Drainage density of the Rorachu river basin was prepared by the method of Euclidean distance in ArcGIS 10.3 into 30 * 30 meter grids (Fig. 5. d). It was classified into five classes by natural breaking method.

Fig. 5. Landslide conditioning factors a. elevation map, b. Slope, c. Soil map and d. Drainage density

3.2.6 Road Density (RD)

In alliance with all the anthropogenic activities are responsible for slope instability, construction and extension of roads networks are major threat in slope instability in mountain areas. Roads modify the natural gradient of the slope and create an obstacle for surface water flow (Marcini, F., 2010). Road map was prepared by different source like, Topographical map and Google Earth. In this Rorachu watershed area, road density was prepared by ArcGIS 10.3 into 30 * 30 meter grid cell (Fig. 6. e).

3.2.7 Normalize Difference vegetation Index (NDVI)

Normalize difference vegetation index (NDVI) is a numerical indicator that uses for the vegetation conditions of the surface. NDVI was calculating by the formula of NDVI = {(NIR – R) / (NIR + R)}, where NIR is the Near Infrared band and R is the Red band of satellite image. In this Rorachu watershed, calculated NDVI by the LANDSAT 8 OLI image in ERDAS 9.2 image processing software (Fig. 6. f) and ranges the NDVI value -0.11 to 0.64. Positive value indicates the healthy vegetation cover in which useful for slope stability and also reduces soil erosion and slope failure. Negative NDVI values delimitate the no vegetation cover in Rorachu watershed areas which is more vulnerable for slop instability and excessive soil erosion and slope failure.

3.2.8 Slope Curvature

Slope curvature is used to indicate the steepness of a curve at a particular point. Slope curvature is significant parameters for landslide susceptibility mapping (Lee and Sambath, 2006 and Greco et al., 2007). In this Rorachu watershed slope curvature was calculated by the ASTER GDEM data (Fig. 6. g). Slope curvature values illustrate the morphology of the topography (Lee and Min, 2001) that has described the surface condition of this Rorachu river basin. Positive curvature values represent a convex slope which is more probable to slope failure and less drainage concentration. Negative curvature values represent as concave slope which has more chance to drainage concentration and less landslide vulnerability. Zero curvature values represent the flat surface. Mathematically, it is the reciprocal of the radius of a circle that is tangent to a point on a curve (Roberts 2001). It helps us to identify the zones that exhibit instinct to landslide vulnerability. The curvature map of this Rorachu watershed was prepared with five classes.

3.2.9 Topographic position index (TPI)

Topographic position index (TPI) is an algorithm in which increasingly used to measure topographic slope positions and automated landform classifications. Topographic position index (TPI) calculation as proposed by (Guisan et al., 1999).TPI is a topographic position classification identifying upper, middle and lower part of the landscape. Positive TPI values represent locations that are higher than the surroundings (ridges) .Negative TPI values represents locations that are lower than the surroundings (valleys).TPI values near zero are either flat areas or constant slope. In this study area TPI was calculated by SAGA GIS software, and the value of TPI ranges in between -63.51 to 65.13. Topographic position index also important factors for the landslide vulnerability assessment analysis (Fig. 6. h).

Fig. 6. Landslide conditioning factors e. Road density f. NDVI g. Curvature h. TPI

3.2.10 Stream power index (SPI)

Stream power index (SPI) is a measured of the erosive power of the flowing water. Calculation of the stream power index (SPI) based on slope and Specific catchment area (SCA). The stream power index (SPI) can be defined as (Moore and Grayson1991):

$$\mathrm{SPI} = \mathrm{As}\tan\beta \qquad (2)$$

Where, as is the specific catchment area (SCA) and β is the local slope gradient measured in degrees, respectively. In this Rorachu watershed SPI values was represented in between 0 and 145.37 and classified into five classes (Fig. 7. i).

3.2.11 Topographic Wetness Index (TWI)

Topographic wetness index (TWI) another important factors for landslide susceptibility modeling. It is commonly used for to quantify of the topographic control or hydrological process. TWI refers to the accumulation of water in a particular point at a time of any grid cell. For the shallow landslide modeling, using the TWI by different researcher (Gokceoglu et al. 2005; and Yilmaz, 2009). In this study area TWI map was prepared by SAGA GIS software using the following equation (3). TWI map was classified into five categories (Fig. 7. j). TWI model (Beven and Kirkby 1979) defined as

$$\mathrm{TWI} = \ln\left(\frac{a}{\tan\beta}\right) \quad (3)$$

Where, a is the cumulative upslope area draining through a point (per unit contour length) and tanβ is the slope angel at the point, which is used to replace approximately the hydraulic gradient under steady state conditions (Poudyal et al., 2010). In the present study, TWI classified into five classes (fig 6 k), which ranges between 5.83 and 15.25.

3.2.12 Land Use Land Cover (LULC)

Land Use Land Cover (LULC) is one of the most important parameters and significant for the role of slope stability and instability. LULC map was derived LANDSAT 8 OLI satellite image (2019) data, and verified by Google earth image and field verification using supervised classification techniques by ERDAS 9.2 software. The land cover by forest area promotes infiltrate and drainage is considered safe to slope failure. Whereas the cultivated land affects the slope stability owing to saturation of covered soil (Devkota et al., 2012). The study area is exhibit various types of land use land cover such as step cultivation, open forest, settlement, bare soil, landslide area, river and dense forest. In the Rorachu watershed most of the LULC covered by Forest (open and dense) 59 % area followed by settlement 3.47 % and bare land 3.23 % (Fig. 7. k).

Fig. 7. Landslide conditioning factors i. Stream power index (SPI), j. TWI, k. LULC and l. Rainfall (mm)

3.2.13 Rainfall

Rainfall is one of the most important factors for landslide in Rorachu watershed areas. In this mountain area abrupt rainfall causes shallow landslide. Rainfall map was prepared by world climatic data and applied Inverse distance weighted (IDW) modeling for the rainfall mapping and classified into 5 categories. Rorachu watersheds represent the ranges between 1847 mm to 3657 mm rainfall (according to http://www.geog.ucsb.edu/~bodo/TRMM/#tif). Maximum rainfall occurrence in between June and august (according to IMD data, Table 4. Fig.7. l).

Table 4. Monthly Rainfall distribution in the East Sikkim area (2009 – 2015). *Source*: Indian Meteorological Department (IMD) Gangtok, Sikkim

3.3 Modelling landslide susceptibility and Risk

This study summarizes the outcomes of landslide susceptibility mapping in the Rorachu watershed, east Sikkim, through GIS techniques. Although there are several bivariate, multivariate statistical approach for landslide susceptibility or slope instability mapping. For this purpose, among various statistical approaches of slope LSM, we have adopted three different approaching statistical models (FR, IV and CF) for this landslide susceptibility analysis. Details of each statistical approach are describing in the following subsections.

3.3.1 Frequency Ratio (FR) Model

Various bivariate statistical methods were applied previously for landslide susceptibility analysis in different parts of the world where frequency ratio (FR) model is too much popular (Luzi et al. 2000; Lee and Choi 2003; Lee and Talib 2005; Porghasemi 2007; Lee and Pradhan 2007; Akgun et al. 2008; Jadda 2009; Pradhan and Lee 2009). Frequency ration (FR) model is a simple statistical method in which to calculate the probabilistic relationship between present landslide and landslide conditioning factors. This model based on the observed relationships between each factor and appeared landslides in this Rorachu watershed. Frequency ratio (FR) model is the ratio

of the probabilities of landslide occurrence to a nonoccurrence for a given attribute (Bonhan – Carter, 1994; Pradhan and Lee 2009). The frequency ration (FR) model can be expressed as:

$$FR = \frac{\frac{Npix(SXi)}{\sum_{i=1}^{m} SXi}}{\frac{Npix(Xj)}{\sum_{j=1}^{n} Npix(Xj)}} \quad (4)$$

Where, *Npix(SXi)* is the number of pixel with landslides within class I of parameter variable *X*, *Npix(Xj)* is the number of pixel within parameter variable *Xj* , m is the number of classes in the parameter variable *Xi*. And N is the number of parameters in the study area (Regmi et al., 2014). The landslide susceptibility index (LSI) can be propagating by summation of each factors of FR value as:

$$LSI = \sum_{ij=1}^{N} FR \quad (5)$$

Where, LSI is the landslide susceptibility index, N is the total number of variables, *ij* is the frequency ratio value of each class and FR is the frequency ratio values. A FR value greater than 1 indicates the higher probability of landslide occurrence and less than the value 1 is indicating the lower probability of landslide occurrence or low correlation. To calculate the frequency ratio (FR) values in all factors are given (Table 5).

3.3.2 Information Value (IV) model

The information value (IV) is a bivariate statistical method that was develops from information theory. Information model employed for the spatial prediction on an event based on the parameter and event relationships. It has been very useful method for landslide susceptibility modeling by determining the influence of parameter. This information value (IV) model was originally introduced by Yin and Yan (1988) and modified slightly by Van Westen (1993). This model was first applied for geological hazard and disaster risk assessment. The information value (IV) can be expressed by:

$$Ii = \log \frac{Si/Ni}{S/N} \quad (6)$$

Where, Ii is the information value (IV), N = total number of data points (Grid cells), S = number of grid cells with landslides, Si = number of grid cells involving the parameter and containing landslide, Ni = number of grid cells involving the parameter. The landslide susceptibility index (LSI) can be represented by the summation of total information value (IV) in a grid cell j is:

$$LSI\ (Ij) = \sum_{i=1}^{M} Xji\ \times Ii \tag{7}$$

$$LSI\ (Ij) = \sum_{i=1}^{M} Xji\ \times log\frac{Si/Ni}{S/N} \tag{8}$$

Where, *Xji* is the value parameter *I, j* = 1, 2, 3……..M: = 1, if parameter *i* exists in grid cell *j* and = 0, if parameter does not exist in grid cell *j*; M = number of parameter considered. The above model was prepared for each class of parameter variables for landslide susceptibility analysis and total calculate total information value (IV) of grid cell of this Rorachu watershed. More the information value (IV) high probability of landslide susceptibility and less the information value (IV) lowers the probability of landslide susceptibility. To calculate the information value (IV) in all variables in (Table 5).

3.3.3 Certainty Factor (CF) model

Certainty factor (CF) is one of the most probabilistic models in used for landslide susceptibility analysis. Certainty Factor (CF) is a probabilistic model that has been applied by different researchers in landslide susceptibility mapping in different parts of the world (Kanungo et al. 2011; Gokceolu et al. 2005). The certainty factor (CF) model is one of the most possible proposed functions that handle and combine different type of data and heterogeneity and uncertainty of the input data. Higher the percentages of landslides correctly predicted, greater the validity of the CF model which is based on the assumptions. Certainty factor (CF) is calculated on the basis of landslide inventory and landslide frequency occurrence probability of each class in thematic layers. The certainty factor as a function of probability was originally proposed by Shortliffe and Buchanan (1975) and modified by Heckerman (1986). The certainty factor (CF) was calculated in the following equations:

$$CF = \begin{cases} \frac{PPa-PPs}{PPa(1-PPs)} & if\ PPa \geq PPs \\ \frac{PPa-PPs}{PPs(1-PPa)} & if\ PPa < PPs \end{cases} \tag{9}$$

Where, CF is the certainty factor, *PPa* is the conditional probability of having a number of landslides in the class 'a' (e.g., forest in land use land cover layer, concave curvature in curvature layer, etc.) and *PPs* is the prior probability of having the total number of landslides in the study area 'A'. The certainty factor (CF) value ranges between +1 to -1. Positive values intimate an increase of certainty whereas negative value corresponding decrease the certainty. A value close to 0 indicates that the prior probability is very similar to conditional probability. The layers are combined brace wise according to the integration rules (Chung and Fabbri 1993; Binaghi *et al.* 1998). The combination of CF values of two thematic layers 'z' is revealed in the following equation as given by Binaghi *et al.* (1998):

$$Z = \begin{cases} x + y - xy\,, & x, y >= 0 \\ \frac{x+y}{1-min(x\,,y\,)} & x, y\ opposite\ sign \\ x + y + xy & x\,, y < 0 \end{cases} \quad (10)$$

The certainty factor (CF) values were calculated in Rorachu watershed by overlaying each factor with the landslide map and computed the landslide frequencies. Every thematic layer reclassified according to their certainty factor (CF) values and amalgamated pairwise to propagate the landslide susceptibility map of Rorachu watershed area using the integrating rule of equation (9). Calculations of certainty factor (CF) in each landslide factors are representing in (Table 5).

Table 5. Spatial relationship between each landslide conditioning factors and observed landslides Using Frequency Ratio (FR), Information Value (IV) and Certainty Factor (CF) models for all landslide causative factors classes.

3.4 Multicollinearity test

Multicollinearity is a statistical testing phenomenon in which one predictor variable in a multiple regression model can be linearly predicted from the others with a substantial degree of accuracy. Multicollinearity does not reduce the predictive power or reliability of the model as a whole; it only effects calculations regarding individual predictors. Before using the landslide causative factors for the landslide susceptibility index (LSI) and landslide risk modeling, it is necessary to

test the multicollinearity of all the landslide causative factors (Zhou et al., 2018; Arabameri et al, 2019; Chen et al., 2018). Tolerance (TOL) and the Variance influencing factors (VIF) are both important indexes for multicollinearity diagnostic. VIF is simply the reciprocal of tolerance (TOL). A tolerance (TOL) of less than 0.20 or 0.10 and/or a VIF of 5 or 10 and above implies a multicollinearity problem (O'Brien 2007). According to the table 6, the smallest tolerance (TOL) of different models (FR, IV and CF) were 0.20, 0.33 and 0.176 showing the elevation parameter respectively. The variance influencing factors (VIF) of these models (FR, IV and CF) are 1.11, 1.16 and 1.109 values showing Road density parameter respectively. So there is no multicollinearity between independent landslide causative factors and current research. The variance influencing factors (VIF) and the tolerance (TOL) as calculated following equations which is as follows

$$TOL = 1 - Ri^2 \quad (11)$$

$$VIF = {}^{1}/_{1 - Ri^2} \quad (12)$$

TOL is the tolerance; VIF is the variance influencing factors and Ri^2 is the coefficient of determination of landslide conditioning factors *i*. The multicollinearity statistics of all the models (FR, IV and CF) are shows in Table 6.

Table 6. Multicollinearity analysis of FR, IV and CF approach.

3.5 Model validation/Performances

The landslide susceptibility mapping was substantiated by different bivariate statistical (FR, IV and CF) model in the Rorachu watershed. Without any proper validations of this statistical model performances are not compatible for landslide susceptibility analysis of any place in the world. The overall ascertainment of the landslide analysis is commonly justified on the number of correctly classified pixels. In this study, the validation process was performed using total observed landslides (716 pixel) are split into two categories 1. 70 % (500) landslides were used for training the model and 2. Remaining 30 % (216) landslides were entrusted for the landslide validations. There exist several approaches for the landslide susceptibility modeling. The

methods are 1. Success rate curve (Van westen et al., 2003; Chung and fabbri, 1999). 2. Landslide density (Gupta et al., 2008; Sarkar and Kanungo, 2004), 3. Spatially agreed area analysis and 4. Receiver operating characteristics (ROC) curve applied different researcher. Here all the validations processes were applied for the proper landslide susceptibility mapping in the Rorachu watershed.

3.6 Landslide Risk (LR) mapping

The risk is the maximum expected degree of loss due to particular landslide events in a particular area and during certain time of period is called landslide risk. Landslide risk assessment (LRA) modeling aims to determine the probability of element-at-risk that a specific hazard will cause harm, and it investigates the relationship between the recurrence of damaging events and the intensity of the consequences (Guzzetti et al. 2009). The risk analysis is very much significant in the mountainous buildings, population and roads for the planning, land use management and other means. There is several researcher used landslide risk analysis (Varnes DJ. 1984; Fell 1994; Leroi 1996; Xu et al., 2012). According to Xu et al. (2012), risk is defined as the probability of damage caused by a particular hazard to a specific element is followed by this equation as

$$Risk = H \times V \quad (13)$$

Here, H denotes the Hazard expressed as probability of occurrence within a reference period and V define the Physical vulnerability of a particular type of element-at-risk (from 0 = not vulnerable and 1 = vulnerable) for a specific type of hazard and for a specific element-at-risk. In order to determine the landslide risk mapping in the Rorachu watershed (Figure 10),

4. Result and Discussion

In the present study, we have used three models for landslide susceptibility analysis in Rorachu watershed areas, 1. Frequency Ratio (FR) model, 2. Information Value (IV) model and 3. Certainty Factor (CF) model. These three models (FR, IV and CF) were used for the slope instability analysis using thirteen aforementioned landslide susceptibility factors. From the analysis we get the following results:

4.1 Frequency Ratio (FR) model, Susceptibility zones and causative factors

The frequency ratio (FR) model has been valuable in ranking the preferred etiological factors based on their efficiency for landslide susceptibility analysis in past few years and, it's widely been used by different researcher throughout the world. In this study we calculate the landslide susceptibility index (LSI), each frequency ratio (FR) values were summed (Lee and min, 2001; Lee and Pradhan, 2007) of each factors as expressed in equation (14). The result LSI map is depicted in (Fig. 8).

$$LSM_{FR} = \sum (FR_{Elevation} + FR_{Geology} + FR_{Slope} + FR_{Soil} + FR_{Drainage\ density} + FR_{Road\ density} + FR_{Rainfall} + FR_{NDVI} + FR_{Curvature} + FR_{TPI} + FR_{SPI} + FR_{TWI} + FR_{LULC}) \quad (14)$$

Therefore the FR values was greater than 1, the stronger the probability of landslide occurrence and vice versa (table 5). To describe the level of correlation between the landslide causative factors and the frequency ratio (FR) model is that where the slope class 45^o to 70^o has the highest value of FR (1.1568) followed by the slope of 35^o to 45^o class has the value of CF (1.4369) whereas the other slope classes has lower FR. As slope angle increases, the shear stress and other unconsolidated material increases. For the curvature factor, convex curvature has the highest FR (1.469) due to the higher erosional activity, road construction in Rorachu watershed and human activity. In case of elevation, class of 3110 – 4100 m has the highest frequency ratio (FR) value of 3.418 and 2516 – 3110 m has the FR (2.251). Below the 2500 m altitude there was less relationship of FR. It indicates that the Rorachu watershed area has very high probability of landslide in above the value of 2500 meters. In this study area geology also important factors for slope instability. For the geology, it can be seen that Chungthang formation (FR = 1.937), Kanchanjangha formation (FR = 1.301), Basic intrusive (FR = 0.357), Gorubathan formation (FR = 0.069) and lingtse gnesis (FR = 0) are found in this Rorachu river basin. In the case of land use land cover, positive value of FR is seen bare soil (FR = 4.076) and open forest (FR = 1.348) and the lowest value seen in settlement (FR = 0) and river (FR = 0).

553 The impression of other factors were also analyze for the landslide susceptibility analysis. For
554 the soil, it can be seen accordingly loamy skeletal (FR = 3.6), coarse loamy (FR = 1.999), coarse
555 loamy holithic (FR = 1.394), coarse loamy distrudeptic (FR = 0.414), fine skeletal (FR = 0.02)
556 and fine loamy (FR = 0). In the case of normalize difference vegetation index (NDVI), the class
557 of -0.111 to 0.142 has represented the highest FR (2.263) value and the high NDVI value
558 represent the lowest FR (0.455) value. The road densities also important for landslide
559 susceptibility, in this study the moderate road density class represent the highest FR (3.203)
560 value and high class represent FR (2.368) value. The lowest road density class has the lowest FR
561 (0.438) value, because of that this Rorachu watershed not only coverage too many roads but also
562 coverage the one state highway in NE position. It May be this state highway one of the major
563 causes for landslide in this Rorachu watershed. The stream power index (SPI) range of low (FR
564 = 1.30) and moderate (FR = 1.23) has the highest positive value, followed by very high (FR = 0)
565 has the lowest probability of landslide. Because of that the highest SPI value observed in the
566 very high elevation where rocks are very compact and hard. The final result of certainty factor
567 (FR) model is landslide susceptibility index (LSI), in which the LSI values ranges between 4.02
568 and 27.1. This map was classified by natural breaking method. According to landslide
569 susceptibility map procreate with the frequency ratio (FR) model by the equation 13 (Fig. 8.
570 Table 5), there was found that 6.10 % and 16.64 % of the total landslides area fall in very high
571 and high susceptible class, respectively. Moderate, low and very low susceptible zones narrate
572 25.30 %, 32.91 % and 19.03 % of the total landslide area, respectively. The high and very high
573 landslide susceptible area includes about 22.74 % of the total susceptible area in the Rorachu
574 watershed.
575
576 Fig. 8. Landslide susceptibility map emanated by frequency ratio (FR) model
577
578 ***4.2 Information Value (IV) model, Susceptibility zones and causative factors***

579 The landslide inventory map was overlaid with the landslide causative factors to dispose the
580 significance of each factor class for landslide occurrence. Using the information value (IV)
581 model, we computed landslide susceptibility map of Rorachu watershed by the equation (15).
582 The final landslide susceptibility map was performed by the IV model is shown (Fig. 9). All the
583 thirteen landslide variables were discerned for the landslide modelling (Table 5).

$$LSM_{IV} = \sum (IV_{Elevation} + IV_{Geology} + IV_{Slope} + IV_{Soil} + IV_{Drainage\ density} + IV_{Road\ density} + IV_{Rainfall} + IV_{NDVI} + IV_{Curvature} + IV_{TPI} + IV_{SPI} + IV_{TWI} + IV_{LULC}) \quad (15)$$

To perform the landslide susceptibility mapping using the information value (IV) model. In the case of slope the majority of landslide probability occurrence in moderate (25^o to 35^0) and high slope (35^o to 45^o) has the highest value of IV (1.51) and IV (1.49) accordingly. However, the IV of gentle slope is lower which implies no effect on slope instability. This IV model indicates the ranges between 25^o to 45^o slope are major probability of landslide in this Rorachu watershed. In terms of slope curvature, the highest (1.74) and lowest (1.12) information value (IV) are located in the slope curvature class of concave and flat area, and also the convex curvature class represent the IV (1.57). In this watershed convex and concave curvature both are uniformly affected by the landslide susceptible area. . The relationship between elevation and the landslide occurrence probability is the highest seeing the 2500 meter to 3110 meters where the information value (IV) is (1.70) and also the highest probability of landslide occurrence is also seeing very high elevation (3110 to 4100 m) where information value (IV) is (1.51). And the elevation between 816 and 1500 m represent the lowest information value (IV) is -0.125. For the geology, it can be seen that Chungthang formation (IV = 1.58), Kanchanjangha formation (IV = 1.77), Basic intrusive (IV = 0.9), Gorubathan formation (IV = -0.04) and lingtse gnesis (IV = 0) are found in this Rorachu watershed. In the case of land use land cover, positive value of IV is seen bare soil (IV = 1.34) and open forest (IV = 1.57) and the lowest value seen in settlement (IV = 0.02).

Fig. 9. Landslide susceptibility map emanated by Information value (IV) model

4.3 Certainty Factor (CF) model, Susceptibility zones and causative factors

Landslide susceptibility map delineate areas, identifying areas with the same probable circumstance of slope failure. In this study we applied certainty factor (CF) model for final landslide susceptibility analysis in Rorachu watershed area (Fig. 10). Certainty factor (CF) is the

probabilistic study in which provides the favorable function value of each class of landslide susceptibility factors. The thematic layers are integrated pairwise using the integration rules (Binaghi et al. 1998). The certainty values were enumerated for all landslides conditioning factors by overlaying and considerate the landslide frequency (Table 5). Then, thirteen landslide conditioning factors were ascertained using Eq. 16. In order to calculate a LSI map (Fig. 10)

$$\left(\begin{aligned} LSM_{CF} = \sum (&CF_{Elevation} + CF_{Geology} + CF_{Slope} \\ &+ CF_{Soil} + CF_{Drainage\ density} + CF_{Road\ density} \\ &+ CF_{Rainfall} + CF_{NDVI} + CF_{Curvature} \\ &+ CF_{TPI} + CF_{SPI} + CF_{TWI} + CF_{LULC}) \end{aligned} \right) \quad (16)$$

It can be observed in (table) the slope class 45° to 70° has the highest value of CF (0.366) followed by the slope of 35° to 45° class has the value of CF (0.307). The lowest value of CF (-0.601) is for slope class 0° to 15°. From this it is clearly indicating that landslides occurrence augmentation by the increases of slope factors upto certain extent, and then, it decreases. Landslide occurrence decreases as the slopes becomes higher then 45° (Devkota, K., 2012) but in this Rorachu watershed occurrence of landslide probability value of CF (0.366) upto 70° slope, and the reason for that is the high human activity, state highway construction and development in that hilly slope. In the case of plane curvature in Rorachu watershed, the convex curvature was representing maximum CF (0.322) value and flat curvature represent the minimum CF (-0.516). That means the landslide probability highest in the convex curvature and concave and flat curvature are not responsible landslides in this area. The relationship between elevation and the landslide occurrence probability is seeing the 3110 meter to 4100 meters where the certainty factor (CF) value is (0.714). And the elevation between 816 m to 1500 m represent the lowest CF (-0.963) and also the positive CF value ranges between 2500 m to 4100 m and negative CF value ranges between 816 m to 2500 m. This shows the probability of landslide occurrence decreases at the altitudes lower than 2500 m in the Rorachu river basin. For the geology, it can be seen that Chungthang formation (CF = 0.488), Kanchanjangha formation (CF = 0.234), Basic intrusive (CF = -0.645), Gorubathan formation (CF = -0.931) and lingtse gnesis (CF = -1) are found in this Rorachu watershed. In the case of land use land cover, positive value of CF is seen bare soil (CF

643 = 0.762) and open forest (CF = 0.261) and the highest negative value seen in settlement (CF = -
644 0.807).
645
646 The impression of other factors were also been analyzing for the landslide susceptibility analysis.
647 The road densities also important for landslide susceptibility, in this study the moderate road
648 density class represent the highest CF (0.694) value and high class represent CF (0.583) value.
649 The lowest road density class has the lowest CF (-0.564) value, because of that this Rorachu
650 watershed not only coverage too many roads but also coverage the one state highway in NE
651 position. It May be this state highway one of the major causes for landslide in this Rorachu
652 watershed. The final result of certainty factor (CF) model is landslide susceptibility index (LSI),
653 in which the LSI values ranges between – 5.98 and 13.58.
654
655 Fig. 10. Landslide susceptibility map emanated by Certainty factor (CF) model
656 Fig. 11. Google earth map showing the very high (VH) and high (H) landslide susceptibility of
657 various models (FR, IV and CF).
658 ***4.3 Results of models validation***
659 ***4.3.1 Landslide Density (LD) method and model's validation***
660 Landslide density is the ratio between the observed landslides in that area and the area of each
661 landslide susceptible classes. In the present study we calculate the landslide density on the basis
662 of the number of landslides pixels having present in this study area and the landslides susceptible
663 map having pixels (table 7). In an ideal landslide susceptible zonation map is where he is called
664 the higher landslide density present in higher landslide susceptibility classes and vice versa.
665 From the table 6, it was conspicuous that landslide densities gradually increases from the low
666 landslide susceptible to class to high susceptible classes. In this study it can be observed that the
667 very high landslide susceptible class represent the highest landslide density values 0.04607 (FR
668 model), 0.021 (IV model) and 0.0403 (CF model). Furthermore, there was a continuous
669 decrement of landslide density values from very high to low landslide susceptibility zonation
670 map and also there was also a considered different landslide density values for different landslide
671 susceptible classes (Fig.12). The comparison of the all three statistical model for landslide
672 susceptibility mapping discloses that the maps produced from two statistical models are
673 noticeably better than that of the information value (IV) model. This may be due to additional

objectivity in the landslide model weight assignment process of the frequency ratio (FR) and certainty factor (CF) method than the information value (IV) method.

Table 7. The comparison between observed landslide and landslide susceptibility model with the landslide density (LD).

Fig. 12. The landslide density (LD) has been showing the increasing trend to the highest vulnerable areas.

4.3.2 Result of Success rate cure (SRC) and models validation

Landslide susceptibility zonation maps can also be validated from the success rate curve (SRC) (Chung and Fabbri, 1999; Van westen et al., 2003) and try to find out the best probable relationship between observed landslides and landslide susceptible zones. The percentage of phenomenon of landslides in any susceptible zones gives the successive rate. In this study area the cumulative percentage of observed landslides plotted against the cumulative percentage of landslide index (LSI) susceptibility zonation map to obtain the successive rate curve (SRC) for each bivariate statistical model of the Rorachu watershed (Fig. 13). in this study the analysis exhibit that the first 20 % of this area comprise about 0.42 %, 2.23 % and 0.41 % of observed landslides for the frequency ratio (FR), Information value (IV) and certainty factor (CF) model and landslide susceptibility index (LSI) respectively. The area under curve (AUC) was assessing for the accuracy of the landslide analysis method qualitatively. In the present study, the areas under curves (AUC) are 0.868, 0.846 and 0.925 which means that the overall success rates are 86.8 %, 84.6 % and 92.5 % for the certainty factor (CF), information value (IV) and frequency ratio (FR) models, respectively. These result also validate the landslide susceptibility mapping in the Rorachu watershed, indicates that the susceptibility maps obtained by the certainty factor (CF), information value (IV) and frequency ratio (FR) models are qualitatively similar or better for the modelling in Rorachu watershed.

Fig. 13. Success rate curve (SRC) for the three models (FR, IV and CF) in the Rorachu watershed

4.3.3 Result of Receive operating characteristics (ROC) curve method and model's validation

An appropriate validation is required to prepare a certain landslide susceptibility map of the study area. In the current study, the validations of the landslide susceptibility map was restrained by receive operating characteristics (ROC) curve (Akgun et al., 2012; Regmi et al., 2014; Ozdemir and Altural, 2013). A receive operating characteristics (ROC) curve is a graphical plot in which illustrate the diagnostic caliber of a binary classifier system as its discrimination threshold is varied. The ROC curve is created by plotting the true positive (TP) rate against the false positive (FP) rate at various threshold settings. The ROC curve is an efficient method for the representing the quality of probability and deterministic detection and forecasting system. The area under curve (AUC) represents the quality of the landslide probabilistic models to feasible predict of the occurrence and non-occurrence of landslides. A proper fit model has an AUC values ranges between 0.5 to 1, while values below 0.5 represent the random fit and less reliable for the landslide susceptibility modelling (Yilmaz 2009a, b)

$$\text{Sensitivity} = TP / (TP + FN) \quad (17)$$

$$\text{Specificity} = TN / (TN + FP) \quad (18)$$

$$\text{Specificity} = 1 - \text{Sensitivity} \quad (19)$$

Generally there were three methods used to validate the model. In this study, the AUC values for the FR model are 0.828 and, we could say that the 82.80 % prediction accuracy for this landslide susceptibility modelling in Rorachu watershed. In the case of information value (IV) model, the AUC curve area is 0.750 and, we could say that the 75 % prediction accuracy for the landslide modeling. In the case of applying certainty factor (CF) model, the AUC curve area is 0.836 and, we could say that 83.60 % prediction accuracy shows the landslide modelling in the Rorachu watershed (Fig 14) with the standard error (FR = 0.016, IV = 0.019 and CF = 0.015) in Table 8. To compare the result of all three bivariate models as quantitatively, the areas under curve (AUC) were recalculated acceptance the total area as 1, which means the perfect probabilistic and deterministic prediction accuracy. In this study, a comparison between FR, IV and CF model and observed landslides were conducted. The all statistical model results show that a strong fit

between landslide susceptibility zonation maps and tangible location landslides in the Rorachu watershed.

Fig. 14. Receive operating characteristics (ROC) curve for FR, IV and CF models.

Table 8. The comprehensive statistics in the various model (FR, IV and CF) of the ROC curve.

4.4 Analysis of landslide risk (LR)

The various bivariate statistical approaches were used. For this purpose, firstly landslide susceptibility or hazard map was emanated by the FR, IV and CF bivariate statistical model. The landslide vulnerability map was produced as vulnerability of settlement and road (vulnerability = 1 and non-vulnerability = 0). Finally, the landslide hazard and landslide vulnerability of which element-at-risk are combined by the equation (13) to obtained final landslide risk map. Based on this method the landslide risk (LR) map was classified into five categories, very low (VL), low (L), moderate (M), high (H) and very high (VH) (Fig. 15). According to the landslide risk assessment (LRA) map of road and settlement, the 9.05% (0.67 km^2), 38.59% (1.32 km^2) and 20.09% (0.67km^2) of the settlement areas occupied very high (VH) risk obtained by FR, IV and CF statistical model, respectively. The 20.72% (0.69 km^2), 40.91% (1.38 km^2) and 18.79% (0.63 km^2) of the road areas brought under control very high (VH) risk attained by FR, IV and CF bivariate statistical model, respectively. It has been observed that, the most of the settlements and road have been built up on very high risk area which is located in east side of the Rorachu watershed. Those high risk areas requirements to be brought to the notice of the public so that can government and people can realize the possibility of future risk vulnerability.

The increasing population pressure has been forcing people to multiplication their activities in mountain areas. In this study the, the landslide risk (LR) analysis have been employed in Rorachu watershed that indicates the 9.05 % (FR), 38.59 % (IV) and 20.09 % (CF) settlement area has been showing the highest landslide risk (LR) probability zone and 20.52 % (FR), 40.91 % (IV) and 18.78 % (CF) road area has the highest landslide risk (LR) probability (Fig. 16). The triggering factors has major role for the landslide susceptibility in this area. In this study area, the NH 31A road is more vulnerable to landslide and landslide risk (LR) zonation map also indicates the highest vulnerability. The population is located in west side is safer than the east side.

Fig. 15. Landslide risk map of two variables (Settlement and Road) by the various models (a) Road risk map by Frequency Ratio (FR) model, (b) Road risk map by Information Value (IV) model, (c) Road risk map by Certainty Factor (CF) model, (d) Settlement risk map by Frequency Ratio (FR) model, (e) Settlement risk map by Information Value (IV) model and (f) Settlement risk map by Certainty Factor (CF) model

Fig. 16. The comparative Bar graph revealing the areal distribution of numerous models (FR, IV and CF) a. observed landslide area situated in various landslide susceptibility zones b. Areal distribution of landslide susceptibility zones c. Areal distribution of Roads in various landslide risk zones (LRZ) d. Areal distribution of Settlement in various landslide risk zones (LRZ).

4.5 Triggering factors

Landslides may be a consequence of several geomorphic, climatic, litho-tectonic and anthropogenic factors. But the fact is that, which factors are leading role for the instance of landslides in any place in the world even in Rorachu watershed. There are several researchers to employ the landslide susceptibility mapping in different part of the world. Many researchers have excellent recite to which factors are more effective for landslide susceptibility mapping or slope instability mapping (Pradhan and Kim 2014; Lee and Min 2001; Melchiorre et al. 2008; Chen et al. 2009). Slope degree is a very important parameter in the slope instability analysis, and it is frequently used in preparing landslide susceptibility maps (Lee and Min 2001; Saha et al. 2005; Gorsevski et al. 2012). Altitude is another frequently conditioning factor for landslide susceptibility analysis because it is controlled by several geologic and geomorphological processes (Gorsevski et al. 2012; Pourghasemi et al. 2012b; Pradhan and Kim 2014). Earthquake and rainfall also an important factor for landslides susceptibility mapping. In this study we considered rainfall, slope and elevation as triggering factors for the landslides susceptibility mapping of Rorachu watershed. In this study area the ultimate probability of landslide vulnerabilities and encumbrance of landslides is related with high altitude, rainfall and slope. In Rorachu watershed, the altitude (2500 – 4110 m), slope (35^{o} – 70^{o}) and rainfall (2300 – 3000

mm) has excessive affect for the landslides. The direct impact of monsoonal rainfall on landslides in this watershed (Fig. 17).

Fig. 17. The probability of landslide vulnerability in various ranges (Elevation, Slope and Rainfall).

Conclusion

Landslides are the profuse numerous natural hazards in all over the world causing significant threat to life and property. Several techniques and statistical models have been used for the landslide susceptibility mapping of Rorachu watershed. The present study demonstrates that FR, IV and CF models are successfully applied for the landslide susceptibility mapping and landslide risk assessment (LRA) mapping in the tectonically active Rorachu watershed. The validations have been determined by using the ROC curve method in which accuracies are showing 82.80 %, 75 % and 83.60 % for the frequency ratio (FR), information value (IV) and certainty factor (CF) models, accordingly. Respectively the success rate curves (SRC) are showing accuracies 92.5 %, 84.6 % and 86.8 %, respectively for predictive rate techniques. In this study the frequency ratio (FR) and certainty factor (CF) models provided better result for this slope instability modeling where information value (IV) models could not provide very much satisfied result for this Rorachu watershed. It highlights the influence of some triggering factors (Geology, Elevation, Slope and rainfall) in which maximum contribution for the slope instability in the Rorachu watershed. The results revel that the probability of slope instability instance is higher for the landslide causative factors in which concentrate in geology (chungthang and kanchanjonga formation), slope (35^o to 70^o), elevation (2000 – 4000 m) and rainfall (1800 – 3000 mm) in this watershed. So we must distinguish attention should be taken into consideration for these factors (geology, slope, elevation, rainfall and earthquake) and the NH 31A constructions and development (urbanization, deforestation,) works in this watershed which has to be special preparations needed. The north and northeast of the Rorachu watershed was generally identified high susceptible to landslides, whilst south and southwest was determine the low susceptible areas. Because the north and northeast side having high slope with lower forest area and orderly human activity with NH31A road construction has been turned to higher probability landslide prone zone and the south and southwest portion of this Rorachu watershed

has low slope with high vegetation cover and lowest human activity turned into a lowest probability landslide susceptibility zones.

The landslide susceptible zonation map revels that the 22.7 % (FR) of the study area lies on very high to high LSI zones in which predicts 76.9 % of the past landslides, 45.6 % (IV) of the study area lies on very high to high LSI zones in which predicts 85.06 % of the past landslides and 31.75 % of the study area lies on very high to high LSI zones map predicts 85.05 % of the past landslides. In this study the, the landslide risk (LR) analysis have been employed in Rorachu watershed that indicates the 9.05 % (FR), 38.59 % (IV) and 20.09 % (CF) settlement area has showing the highest landslide risk (LR) probability zone and 20.52 % (FR), 40.91 % (IV) and 18.78 % (CF) road area has the highest landslide risk (LR) probability (fig 13). In this study such results can be used for the mitigating hazard associated with the landslides in this Rorachu watershed. This susceptibility map of Rorachu watershed can be used in future for slope management, land use planning, urban planning, disaster management planning and road construction, etc., by the concerned authorities. The landslide risk (LR) map will help for the producing sustainable products; maintain site equality and sustainably reducing the risk of this settlement and road of any adverse impact.

Conflicts of interest

The authors declare that they have no competing interests

REFERENCE

Arabameri A, Pradhan B, Rezaei K, Sohrabi M, & Kalantari Z (2019) GIS-based landslide susceptibility mapping using numerical risk factor bivariate model and its ensemble with linear multivariate regression and boosted regression tree algorithms. J Mt Sci, 16(3), 595-618.

Akgun A, Dag S, Bulut F (2008) Landslide susceptibility mapping for a landslide-prone area (Findikli, NE of Turkey) by likelihood frequency ratio and weighted linear combination models. Environ Geol 54(6):1127–1143

Akgun A, Turk N (2010) Landslide susceptibility mapping for Ayvalik (Western Turkey) and its vicinity by multi-criteria decision analysis. Environ Earth Sci. 61, 595–611.

Akgun A, Sezer EA, Nefeslioglu HA, Gokceoglu C, Pradhan B (2012) An easy-touse MATLAB program (MamLand) for the assessment of landslide susceptibility using a Mamdani fuzzy algorithm. Comput Geosci 38 (1), 23–34.

Aleotti P, Chowdhury R (1999) Landslide hazard assessment: summary review and new perspectives. Bull Eng Geol Environ 58(1):21–44'

Ayalew L, Yamagishi H, Maruib H, Takami K (2005) Landslide in sado island of japan: part II. GIS-based susceptibility mapping with comparisons of results from two methods and verifications. Eng Geol 81(4):432-445

Ayalew L, Yamagishi H (2005) the application of GIS-based logistic regression for landslide susceptibility mapping in the Kakuda Yahiko Mountains, Central Japan. Geomorphology 65:15–31

Beven KJ, Kirkby MJ (1979) A physically based, variable contributing area model of basin hydrology. Hydro Sci Bull 24:43–69

878

879 Bhasin R, E. Grimstad, J Larsen, AK Dhawan, R Singh, SK Verma, and K
880 Venkatachalam (2002) "Landslide Hazards and Mitigation Measures at Gangtok, Sikkim
881 Himalaya." Engineering Geology 64: 351–368. doi:10.1016/S0013-7952(01)00096-5.
882
883 Binaghi E, Luzi L, Madella P, Pergalani F, Rampini A (1998) Slope instability zonation: a
884 comparison between certainty factor and fuzzy Dempster–Shafer approaches. Nat
885 Hazards 17:77–97
886
887 Bonham – Carter GF (1994) Geographic information systems for geoscientists: modelling with
888 GIS. In: Bonham – Carter F(ed) Computer methods in geosciences. Pergamon, Oxford p
889 398
890
891 Bui DT, Pradhan B, Lofman O, Revhaug I, Dick OB (2012a) Landslide susceptibility assessment
892 in the Hoa Binh province of Vietnam using artificial neural network. Geomorphology.
893 doi:10.1016/ j.geomorph.2012.04.023
894
895 Cevik E, Topal T (2003) GIS-based landslide susceptibility mapping for a problematic segment
896 of the natural gas pipeline, Hendek (Turkey). Environ Geol 44:949–962
897
898 Choubey, VD (1992) "Landslide Hazards and their Mitigation in the Himalayan Region".In
899 Proceedings of the Sixth International Symposium on Landslide, 1849–1868.
900 Christchurch, New Zealand, February 10–14.
901
902 Claessens L, et al (2006) Contribution of topographically based landslide hazard modeling to
903 the analysis of the spatial distribution and ecology of kauri (Agathisaustralis). Landscape
904 Ecol. 21, 63–76.
905
906 Carrara A, CardinaliM, Guzzeti F, Reichenbach P (1995) GIS technology in mapping landslide
907 hazard. In: Carrara A, Guzzetti F (eds) Geographical information systems in assessing

natural hazards. Kluwer Academic Publishers, Dordrecht, pp 135–175

Chen W, Shahabi H, Shirzadi A., Hong H, Akgun A, Tian Y, Liu J, Zhu A, & Li S, (2018) Novel hybrid artificial intelligence approach of bivariate statistical-methods-based kernel logistic regression classifier for landslide susceptibility modeling, Bull Eng Geol Environ. (2019) 78:4397–4419 https://doi.org/10.1007/s10064-018-1401-8

Chung CF, and Fabbri AG (1993) The representation of geosciences information for data integration; *Non-renewable Resour.* **2(2)** 122–139.

Choi J, et al (2011) Combining landslide susceptibility maps obtained from frequency ratio, logistic regression, and artificial neural network models using ASTER images and GIS. Eng. Geol. 124, 12–23.

Chowdhury RN (1976) Initial stresses in natural slope analysis, rock engineering for foundations and slopes. ASCE Geotechnical Engineering Specialty Conference, Boulder, Colorado, pp 404–414 Chowdhury RN, Bertoldi C (1977) Residual shear tests on soil from two natural slopes. Australian Geomechanics Journal G7:1–9

CRED (2009) Centre for Research on the Epidemiology of Disasters (CRED) website. http:// www.dmdat.be/

Dahal RK, Hasegawa S, Nonomura A, Yamanaka M, Takuro M, Nishino K (2008) GIS-based weights-ofevidence modelling of rainfall-induced landslides in small catchments for landslide susceptibility mapping. Environ Geol 54:311–324

Dai F, Lee C, Li J, and Xu Z (2001) Assesment of landslides susceptibility on the natural terrain of lantau Island, Hong Kong. Environmental Geology, 40, 381-391.

Demir G, Aytekin M, Akgun A, Ikizler SB, Tatar O (2012) A comparison of landslide susceptibility mapping of the eastern part of the North Anatolian Fault Zone (Turkey) by

likelihood-frequency ratio and analytic hierarchy process methods. Nat Hazards. doi:10.1007/s11069-012-0418-8

Devkota K, Regmi AD, Pourghasemi HR, Yishida K, Pradhan B, Ryu IC, Dhital MR, althuwaynee OF (2012) Landslide susceptibility mapping using certainty factor. Index of entropy and logistic regression models in GIS and their comparision at Mugling – Narayanghat road section in Nepal Himalaya. Nat Hazards.

Ercanoglu M, Gokceoglu C (2004) Use of fuzzy relations to produce landslide susceptibility map of a landslide prone area (West Black Sea Region, Turkey). Eng Geol 75:229–250

Ercanoglu M, Kasmer O, Temiz N (2008) Adaptation and comparison of expert opinion to analytical hierarchy process for landslide susceptibility mapping. Bull Eng. Geol. Environ. 67, 565–578.

Fell R (1994) Landslide risk assessment and acceptable risk. Can Geotech J 31:261– 272

Greco R, Valvo MS, Catalano E (2007) Logistic Regression analysis in the evaluation of mass movement's susceptibility: the Aspromonte case study, Calabria, Italy. Eng. Geol. 89, 41 66.

Guisan A, Weiss SB, Weiss AD (1999) GLM versus CCa spatial modeling of plant species distribution. Plant Ecology 143: 107-122

Gupta S, H Kaur, S Parkash, and R. Thapa (2018) "Landslide Susceptibility Zonation of Gangtok city, Sikkim using Knowledge Driven Method (KDM)." Disaster Advances 11 (11): 34–43.

Gupta, RP, Kanunga DP, Arora MK, and Sarkar S (2008) Approaches for comparative evolution of raster GIS-based landslide susceptibility zonation maps. Internat. Jour. Appld. Earth Observations and geofinformation, v.10, pp.330-341.

Guzzetti F, Carrara A, Cardinali M, Reichenbach P (1999) Landslide hazard evaluation: a review

970 of current techniques and their application in a multi-scale study, Central Italy.
971 Geomorphology 31:181– 216
972 Guzzetti F, Reichenbach P, Ardizzone F, Cardinali M, & Galli M (2009). Landslide hazard
973 assessment, vulnerability estimation and risk evaluation. An example from the
974 Collazzone Area (Central Umbria, Italy). Geogr Fis Dinam Qual, 32, 183–192.
975
976 Gokceoglu C, Aksoy H (1996) Landslide susceptibility mapping of the slopes in the residual
977 soils of the Mengen region (Turkey) by deterministic stability analyses and image
978 processing techniques. Eng Geol 44:147–161
979
980 Gokceolu C, Sonmez H, Nefeslioglu HA, Duman TY, Can T (2005) The 17 March 2005 Kuzulu
981 landslide (Sivas, Turkey) and landslide-susceptibility map of its near vicinity. Eng Geol
982 81:65–83
983
984 Gorsevski PV, Donevska KR, Mitrovski CD and Frizado JP (2012) integrating multi-criteria
985 evaluation techniques with geographic information systems for landfill site selection: A
986 case study using ordered weighted average; Waste Management 32(2) 287–296.
987
988 Heckerman D (1986) Probabilistic interpretation of MYCIN's certainty factors. In: *Uncertainty*
989 *in Artificial Intelligence* (eds) Kanal L N and Lemmer J F (Dordrecht: Kluwer Academic
990 Publishers), pp. 167–196.
991
992 Horton RE (1932) Drainage basin characteristics. Trans. Am. Geophys. Union 13, 350–361.
993 Horton RE (1945) Erosional development of streams and their drainage basins: a hydro
994 physical approach to quantitative morphology. Geol. Soc. Am. Bullet. 56, 275–370.
995
996 Jadda M (2009) Landslide susceptibility evaluation and factor effect analysis using probabilistic-
997 frequency ratio model. Eur J Sci Res 33(4):654–668
998
999 Jaafari A, Najafi A, Pourghasemi HR, Rezaeian J, and Sattarian A (2014) GIS-based frequency
1000 ratio and index of entropy models for landslide susceptibility assessment in the Caspian

forest, northern Iran; Int. J. Environ. Sci. Tech. 11(4) 909–926.

Kaur H, S. Gupta, and S. Parkash (2017a) "Comparative Evaluation of Various Approaches for Landslide Hazard Zoning: A Critical Review in Indian Perspectives." Spatial Information Research 25: 389–398. doi:10.1007/s41324-017- 0105-7.

Kanungo DP, Arora MK, Sarkar S, Gupta RP (2006) A comparative study of conventional, ANN black box, fuzzy and combined neural and fuzzy weighting procedures for landslide susceptibility zonation in Darjeeling Himalayas. Eng Geol 85:347–366

Kanungo DP, Arora MK, Gupta RP, Sarkar S (2008) Landslide risk assessment using danger pixel and fuzzy concepts in Darjeeling Himalayas. Landslides 5:407–416

Kanungo DP, Sarkar S, Sharma S (2011) Combining neural network with fuzzy, certainty factor and likelihood ratio concepts for spatial prediction of landslides. Nat Hazards 59:1491–1512

Komac M, 2006. A landslide susceptibility model using the analytical hierarchy process method and multivariate statistics in perialpine Slovenia. Geomorphology 74 (1–4), 17–28.

Lee S, Min K, (2001) Statistical analysis of landslide susceptibility at Yongin, Korea. Environ. Geol. 40, 1095–1113.

Lee S, Pradhan B (2007) Landslide hazard mapping at Selangor, Malaysia using frequency ratio and logistic regression models. Landslides 4(1):33–41

Lee S, Sambath T (2006) Landslide susceptibility mapping in the Damrei Romel area, Cambodia using frequency ratio and logistic regression models. Environ Geol 50:847–855

Lee S, Talib JA (2005) Probabilistic landslide susceptibility and factor effect analysis. Environ Geol 47:982–990

1032 Lee S, Ryu JH, Min K, Won JS (2003) Landslide susceptibility analysis using artificial neural
1033 network at Boun, Korea. Environ Geo 44:820–833
1034 Lee S, Choi J, Min K (2004) Probabilistic landslide hazard mapping using GIS and remote
1035 sensing data at Boun, Korea. Int J Remote Sens 25:2037–2052
1036
1037 Lee S (2007a) Comparison of landslide susceptibility maps generated through multiple logistic
1038 regression for three test areas in Korea. Earth Surf Proc & Landf 32:2133–2148
1039
1040 Lee S (2007b) Application and verification of fuzzy algebraic operators to landslide
1041 susceptibility mapping. Environ Geol 52:615– 623
1042
1043 Lee S, Pradhan B (2006) Probabilistic landslide hazards and risk mapping on Penang Island,
1044 Malaysia. J Earth Syst Sci 115:661–672
1045
1046 Lee S, Pradhan B (2007) Landslide hazard mapping at Selangor Malaysia using frequency
1047 ratio and logistic regression models. Landslides 4, 33–41.
1048
1049 Lee S, Ryu JH, Kim IS (2007) Landslide susceptibility analysis and its verification using
1050 likelihood ratio, logistic regression, and artificial neural network models: case study o
1051 Youngin, Korea. Landslides 4, 327–338.
1052
1053 Lee S, Sambath T (2006) Landslide susceptibility mapping in the Damrei Romel area, Cambodia
1054 using frequency ratio and logistic regression models. Environ Geol 50(6):847–855
1055
1056 Leroi E (1996) Landslide hazard—risk maps at different scales: objectives, tools and
1057 development. In: Senneset K (eds) Landslides—Glissements de Terrain, 7th International
1058 symposium on landslides. Balkema, Trondheim, Norway, pp 35–51
1059
1060 Lin CW, SH Liu, SY Lee, and CC Liu (2006) “Impacts of the Chi-Chi Earthquake on
1061 Subsequent Rainfall-Induced Landslides 463 in Central Taiwan.” Engineering Geology
1062 86 (2–3): 87–101. doi:10.1016/j.enggeo.2006.02.010.

Luzi L, Pergalani F, Terlien MTJ (2000) Slope vulnerability to earthquake at subregional scale, using probabilistic techniques and geographic information systems. Eng Geol 58:313–336

Mandal, S, Maiti R (2013) Integrating the Analytical Hierarchy Process (AHP) and the Frequency Ratio (FR) model in landslide susceptibility mapping of Shiv-khola Watershed, Darjeeling Himalaya. Int. J. Disaster Risk Sci. 4 (4), 200–212. https://doi.org/10.1007/s13753-013- 0021-y.

Mandal S, Maiti, R (2015) Semi-quantitative Approaches for Landslide Assessment and Prediction. Part of the series. Springer Natural Hazards.

Mandal S, Mandal K (2017a) Bivariate statistical index for landslide susceptibility mapping in the Rorachu river basin of eastern Sikkim Himalaya, India. Spat Inf Res 26(1):59–75

Marcini, F, Ceppi C, & Ritrovato G (2010). GIS and statistical analysis for landslide susceptibility mapping in the Daunia area, Italy. Natural Hazards Earth System Science, 10, 1851–1864. https://doi.org/10.5194/nhess-10-1851-2010.

Melchiorre C, Matteucci M, Azzoni A, Zanchi A (2008) Artificial neural networks and cluster analysis in landslide susceptibility zonation. Geomorphology 94:379–400

Muthu K, Petrou M, Tarantino C, Blonda P (2008) Landslide possibility mapping using fuzzy approaches. IEEE Trans Geosci Remote Sens 46(4):1253–126

Mohammady M, Pourghasemi HR, Pradhan B (2012) Landslide susceptibility mapping at Golestan Province, Iran: a comparison between frequency ratio, Dempster-Shafer, and weights of-evidence models. J Asian Earth Sci 61:221–236

Moore ID, Grayson RB, Ladson AR (1991) Digital terrain modelling-a review of hydro-

hydrological, geomorphological, and biological application. Hydrol. Process 5, 3–30.

Naithani A (1999). The Himalayan landslides. Employment News, 23(47), 20–26 Oh HJ, Lee S, Chotikasathien W, Kim CH, Kwon JH (2009) Predictive landslide susceptibility mapping using spatial information in the Pechabun area of Thailand. Environ Geol 57:641–651

Oh HJ, Lee S (2011) Landslide susceptibility mapping on Panaon Island, Philippines using a geographic information system. Environ Earth Sci 62:935–951

Ozdemir A (2009) Landslide susceptibility mapping of vicinity of Yaka Landslide (Gelendost, Turkey) using conditional probability approach in GIS. Environ Geol 57:1675–1686

Ozdemir A, Altural T (2013) A comparative study of frequency ratio, weights of evidence and logistic regression methods for landslide susceptibility mapping: Sultan Mountains, SW Turkey. J Asian Earth Sci 64:180–197

Poudyal CP, Chang C, Oh HJ, Lee S (2010) Landslide susceptibility maps comparing frequency ratio and artificial neural networks: a case study from the Nepal Himalaya. Environ Earth Sci 61:1049–1064

Pourghasemi HR, Pradhan B, Gokceoglu C, Mohammadi M, Moradi HR (2012a) Application of weights-of evidence and certainty factor models and their comparison in landslide susceptibility mapping at Haraz watershed, Iran. Arab J Geosci. doi:10.1007/s12517-012-0532-7

Pourghasemi HR (2008) Landslide hazard assessment using fuzzy logic (case study: a part of Haraz Watershed). M.Sc Thesis, Tarbiat Modarres University International Campus, Iran, 92 p.

1125 Pradhan B (2010c) Landslide susceptibility mapping of a catchment area using frequency ratio,
1126 fuzzy logic and multivariate logistic regression approaches. J Indian Soc Remote Sens
1127 38(2):301–320
1128
1129 Pradhan B, Lee S (2009) Landslide risk analysis using artificial neural network model focusing
1130 on different training sites. I J Physical Sci 3(11):1–15
1131 Pradhan B, Pirasteh S (2010) Comparison between prediction capabilities of neural network and
1132 fuzzy logic techniques for landslide susceptibility mapping. Disaster Adv 3(2):26–34
1133
1134 Pourghasemi HR, Pradhan B, Gokceoglu C and Moezzi KD (2012b) Landslide susceptibility
1135 mapping using a spatial multi criteria evaluation model at Haraz Watershed, Iran; In:
1136 Terrigenous Mass Movements, Springer-Berlin Heidelberg, pp. 23–49.
1137
1138 Pourghasemi HR, Pradhan B, Gokceoglu C (2012c) Application of fuzzy logic and analytical
1139 hierarchy process (AHP) to landslide susceptibility mapping at Haraz watershed, Iran.
1140 Nat Hazards 63 (2):965–996. Doi:10.1007/s11069-012-0217-2
1141
1142 Pradhan B, Lee S (2010a) Delineation of landslide hazard areas on Penang Island, Malaysia, by
1143 using frequency ratio, logistic regression, and artificial neural network models. Environ
1144 Earth Sci 60(5): 1037–1054
1145
1146 Pradhan B, Lee S (2010b) Landslide susceptibility assessment and factor effect analysis: back-
1147 propagation artificial neural networks and their comparison with frequency ratio and
1148 bivariate logistic regression modeling. Environ Model Softw 25(6):747–759
1149
1150 Pradhan B, Buchroithner MF (2010) Comparison and validation of landslide susceptibility maps
1151 using an artificial neural network model for three test areas in Malaysia. Environ Eng
1152 Geosci 16 (2):107–126
1153
1154 Pradhan B (2010c) Application of an advanced fuzzy logic model for landslide susceptibility
1155 analysis. Int J Comput Intell Syst 3:370– 381

Pradhan B (2011a) Manifestation of an advanced fuzzy logic model coupled with geoinformation techniques for landslide susceptibility analysis. Environ Ecol Stat 18(3):471–493. doi:10.1007/ s10651-010-0147-7

Pradhan B (2011b) Use of GIS-based fuzzy logic relations and its cross application to produce landslide susceptibility maps in three test areas in Malaysia.

Pradhan A M S and Kim Y T (2014) Relative effect method of landslide susceptibility zonation In weathered granite soil: A case study in Deokjeok-ri Creek, South Korea; Nat. Hazards 72(2) 1189–1217.

Rautela P, Lakhera RC (2000) Landslide risk analysis between Giri and Tons Rivers in Himachal Himalaya (India). Int J Appl Earth Obs Geoinf 2:153–160

Regmi AD, Yoshida K, Pradhan B, Pourghasemi HR, Khumamoto T, Akgun A (2014) Application of frequency ratio, statistical index and weights-of-evidence models, and their comparison in landslide susceptibility mapping in Central Nepal Himalaya. Arab J Geosci. doi:10.1007/s12517-012-0807-z

Raman R, Punia M (2012) The application of GIS-based bivariate statistical methods for landslide hazards assessment in the upper Tons river valley, Western Himalaya, India. Georisk Assess Manag Risk Eng Syst Geohazards 6(3):145–161

Rawat MS and Joshi V (2016) Landslide hazard zonation in Rorachu sub watershed of eas district of Sikkim, India, conference paper

Saha AK, et al (2005) An approach for GIS based statistical landslide susceptibility zonation with a case study in the Himalayas. Landslides 2, 61–69.

Sarkar S, and Kanungo DP (2004) An integrated approach for landslides susceptibility

mapping using remote sensing and GIS. Photogrammetric Engineering and Remote Sensing, v.70(5), pp.617-625.

Sahabi H, Hhezri S, Ahmha B.B, and Hashim M. (2014) Landslide susceptibility mapping at central Zab basin, Iran: A comparision between analytical hierarchy process, Frequency ratio and logistic regression models. Catena, 115, 55-70

Shortliffe EH, and Buchanan, GG (1975) A model of inexact reasoning in medicine; Mathematical Biosci. 23 351–379.

Soeters R, van Westen CJ (1996) Slope instability recognition, analysis and zonation. In: Turner KT, Schuster RL (Eds.) Landslide: investigation and mitigation. Special Report 247. Transportation Research Board, National Research Council, Washington DC, 129–177.

Solaimani K, Mousavi SZ, Kavian A (2013) Landslide susceptibility mapping based on frequency ratio and logistic regression models. Arab J Geosci 6:2557–2569

Strahler AN, (1952) Hypsometric (area-altitude) analysis of erosional topography. Geol. Soc. Am. Bullet. 63, 117–142.

Tien Bui D, Lofman O, Revhaug I, Dick O (2011a) Landslide susceptibility analysis in the Hoa Binh province of Vietnam using statistical index and logistic regression. Nat Hazards 59:1413 1444

Tazik E, et al (2014) Landslide susceptibility mapping by combining the three methods fuzzy logic, frequency ratio and analytical hierarchy process in Dozain basin. The International Archives of the Photogrammetry, Remote Sensing and Spatial Information Sciences, Volume XL-2/W3, 2014, In 1st ISPRS International Conference on Geospatial Information Research, 15–17 November 2014 (Iran: Tehran).

Varnes DJ (1984) International association of engineering geology commission on landslides and

1218 other mass movements on slopes: landslide hazard zonation: a review of principles and
1219 practice.UNESCO, Paris, p 63.
1220
1221 Varnes DJ (1984) Landslide hazard zonation: a review of principles and practice. United
1222 Nations International, Paris
1223
1224 Van Westen C (1997) Statistical landslide hazard analysis. ILWIS 2.1 for Windows application
1225 guide. ITC Publication, Enschede, pp 73–84
1226
1227 Van Westen, CJ, Rengers N, and Soeters R (2003) Use of geomorphological information in
1228 indirect landslides susceptibility assessment, natural Hazards, v.30, pp.399-419.
1229
1230 Wang H, Liu G, Xu W, Wang G (2005) GIS-based landslide hazard assessment: an overview.
1231 Prog Phys Geogr 29(4):548–567
1232
1233 Wan S, Lei TC, Huang PC, Chou TY (2008) Knowledge rules of debris flow event: a case study
1234 for investigation ChenYu Lan River Taiwan. Eng Geol 98:102–114
1235
1236 Westen van CJ (1993) Application of geographical information system to landslide hazard
1237 zonation. ITC, International institute for aerospace and earth res. surv. ITC Publication.
1238 Enschede, The Nethelands
1239
1240 Wu WM, Sidle RC (1995) A distributed slope stability model for steep forested basins. Water
1241 Resour Res 31:2097–2110
1242
1243 Wu Z, Wu Y, Yang Y, Chen F, Zhang N, Ke Y, et al. (2017). A comparative study on the
1244 landslide susceptibility mapping using logistic regression and statistical index models.
1245 Arabian Journal of Geosciences, 10, 187. https://doi.org/10.1007/ s12517-017-2961-9.
1246
1247 Xie M, Esaki T, Zhou G (2004) GIS-based probabilistic mapping of landslide hazard using a
1248 three dimensional deterministic model. Nat. Hazards 33, 265–282.

Xu C, Xu X, Lee YH, Tan X, Yu G, Dai F (2012c) The 2010 Yushu earthquake triggered landslide hazard mapping using GIS and weight of evidence modeling. Environ Earth Sci 66(6):1603–1616

Xu CF, Dai X, Xu, and YH Lee (2012) "GIS-based Support Vector Machine Modeling of Earthquake-Triggered Landslide Susceptibility in the Jianjiang River Watershed, China." Geomorphology 145: 70–80. doi:10.1016/j.geomorphology.2011.12.040.

Yalcin A (2008) GIS-based landslide susceptibility mapping using analytical hierarchy process and bivariate statistics in Ardesen (Turkey): comparisons of results and confirmations. Catena 72, 1–12.

Yilmaz I (2010) Comparison of landslide susceptibility mapping methodologies for Koyulhisar, Turkey: conditional probability, logistic regression, artificial neural networks, and support vector machine. Environ Earth Sci 61:821–836

Yilmaz I (2009a) A case study from Koyulhisar (Sivas-Turkey) for landslide susceptibility mapping by artificial neural networks. B Eng Geol Environ 68:297–306

Yilmaz I (2009b) Landslide susceptibility mapping using frequency ratio, logistic regression, artificial neural networks and their comparison: a case study from Kat landslides (Tokat-Turkey). Comput Geosci 35:1125–1138

Yilmaz I (2010a) Comparison of landslide susceptibility mapping methodologies for Koyulhisar, Turkey: conditional probability, logistic regression, artificial neural networks, and support vector machine. Environ Earth Sci 61:821–836

Yilmaz I (2010b) The effect of the sampling strategies on the landslide susceptibility mapping by conditional probability and artificial neural networks. Environ Earth Sci 60:505–519

Yin KJ, and Yan TZ (1988) Statistical prediction model for slope instability of

metamorphosed rocks. Proceedings of the 5th international symposium on landslides, Lausanne, Switzerland, v.2, pp.1269–1272

Zare M, Pourghasemi HR, Vafakhah M, Pradhan B (2012) Landslide susceptibility mapping at Vaz watershed (Iran) using an artificial neural network model: a comparison between multi-layer perceptron (MLP) and radial basic function (RBF) algorithms. Arab J Geosci. doi:10.1007/s12517-012-0610-x

Zezere JL (2002) Landslide susceptibility assessment considering landslide typology, a case study in the area north of Lisbon (Portugal). Nat. Hazards Earth Syst. Sci. 2, 73–82.

Zhang J, CJ van Westen, H Tanyas, O Mavrouli, Y Ge, S Bajrachary, DR Gurung, MR Dhital, and NR Khanal (2018) "How Size and Trigger Matter: Analyzing Rainfall- and Earthquake-Triggered Landslide Inventories 2 and Their Causal Relation in the Koshi River Basin, Central Himalaya." Natural Hazards Earth System Sciences. doi:10.5194/nhess-2018-109.

Zhou C, Yin K, Cao Y, Ahmed B, Li Y, Catani F, & Pourghasemi H R (2018) Landslide susceptibility modeling applying machine learning methods: A case study from Longju in the Three Gorges Reservoir area, China. Computers & geosciences, 112, 23-37.

Zorn M, Komac B (2004) Deterministic modeling of landslide and rockfall risk. Acta Geographica Slovenica 44, 53–100.

1311 Table 1. Sources of data layers of various landslide causative factors

1312

feature layer	source	thematic data layer	resolution
Topographical map	Survey of India, Kolkata. Map no. 78A/11,	Drainage Density	1:50,000
Google Earth image	http://www.earth.google.com	Road Density	30 * 30 m
Geological map	Geological survey of India (GSI)	Geological map	1:250,000
Soil map	NBSS & LUP Regional Centre, Kolkata	Soil map	1:400,000
LANDSAT 8 OLI	http://www.earthexplorer.usgs.gov	Land Use Land Cover (LULC) map NDVI map	30 * 30 m 30 * 30 m
Rainfall data	http://www.worldclim.org	Rainfall Distribution map	1 km * 1 km
ASTER GDEM	http://www.earthexplorer.usgs.gov	Elevation map Slope map Topographic Wetness Index(TWI) map Topographic Position Index(TPI) map Stream Power Index(SPI) map	30 * 30 m 30 * 30 m 30 * 30 m 30 * 30 m 30 * 30m
Topographical map, Google earth image, Satellite data and GPS survey	Field study using GPS and internet	Landslide Inventory map	

1313

1314

1315

1316

1317

1318

1319

1320

1321

1322 Table 2. Description of geological parameters of Rorachu watershed

ERA	FORMATION	CHARACTERISTICS	LITHOLOGY
Meso-Proterozoic	Lingtse gneiss	The gneisses are sheet like bodies of coarse to medium grained, foliated to strongly lineated granite mylonite. These are streaky, banded, augen gneisses or porphyroblastic gneisses and are traversed by concordant and discordant pegmatite veins. Amphibolite intrusives with sharp contacts are also recorded within gneisses. The most characteristic feature of the Lingtse granite is the presence of a stretching lineation.	Granite gneiss (mylonite)
Proterozoic (Undifferentiated)	Basic intrusive	Basic Intrusive rocks are characterized by large crystal sizes, and as the individual crystals are visible, the rock is called phaneritic. This is formed as the magma cools underground and while cooling may be fast or slow; cooling is slower than on the surface, so larger crystals grow.	Tourmaline / biotite leuco granite, schroll rock/ pegmatite, aplite (Undifferentiated)
	Gorubathan formation	The formation consists of mappable, monotonous sequence of inter banded chlorite sericite schist / phyllite, quartzite, meta greywacke, pyritiferrous black slate/ carbon phylllite, basic meta volcanics. Chlorite phyllite is dark green to light green whereas the quartz chlorite phyllite is only light green in color.	Interbanded chlorite-sericite schist / phyllite and quartzite, meta-greywacke (quartzo feldspathic greywacke), pyritiferous black slate, biotite phyllite / mica schist, biotite quartzite, mica schist with garnet, with / without staurolite, chlorite quartzite
	Kanchenjunga gneiss/Darjeeling gneiss	The gneisses, dominantly comprising quartz, feldspar and biotite (with minor amounts of other minerals) have been classified into three types, ie.1) banded / streaky gneisses / migmatites, 2) augen bearing biotite gneiss with/without garnet, kyanite, sillimanite and 3) sillimanite granite gneisses. Mapping of these rocks as individual units is very difficult	Banded / streaky migmatite, augen bearing (garnet) biotite gneiss with/ without kyanite, sillimanlte with palaeosomes of staurolite, kyanite, mica schist, biotite gneiss, sillimanite granite gneiss

		because they are characterized by frequent interchanging and gradational features among themselves.	
	Chungthang formation	The main rock types of this formation are quartzites, garnet-kyanite-staurolite bearing biotite schist, calc silicate rock, graphitic schist and amphibolite.	Quartzite 2. Garnet kyanite sillimanite biotite schist / Garnetiferous mica schist Chungthang 3. Calc-silicate, carbonaceous schist Formation

1323

1324 Table 3. Soil characteristics map of Rorachu watershed (According to Mandal S, Mandal K
1325 2017a)

Mapping unit	Soil name	Soil code	characteristics
Inceptisols	Coarse loamy humic dystrudepts	S001	Very deep, well drained, moderately rapid permeable coarse loamy soil is found in structural benches and Foot slope of mountain associated with moderately shallow to deep, little stony, excessively drained coarse loamy soil with moderate erosion
	Coarse loamy humic Pachic dystrudepts	S002	Moderately rapid permeability is occurred in upland slopes associated with moderately deep, well drained coarse loamy soil with medium run-off, , little stony, excessively drained fine loamy soils with moderate erosion
	Coarse loamy typic hapludolls	S003	Excessively drained, deep coarse loamy soil having little stoniness and slight to moderate erosion is found mainly in the ridges associated with moderate deep to deep coarse loamy soil with little stoniness and moderate erosion
	Fine-loamy fluventic eutrudepts	S004	moderate permeability with Moderately shallow to deep, well drained fine loamy soil is found in steep slope, moderately high saturated hydraulic conductivity and moderate erosion associated with very deep, well drained fine loamy upland soils
Mollisols	Fine-skeletal cumilic hapludolls	S005	Moderately deep to very deep, excessively drained soils with gravelly surface, little stoniness and moderate erosion is found in very steep slope associated with moderately shallow to deep, slight stoniness, excessively drained, moderately erosion prone coarse loamy soil
	Loamy skeletal entic hapludolls	S006	Excessively drained, gravelly loamy soil mainly found in very steep hill side with small stoniness and moderate erosion associated with moderately shallow to deep, slight stoniness, moderately deep to deep, excessively drained, moderately erosion prone gravelly loamy soil

1326

1327

1328 Table 4. Monthly Rainfall distribution in the East Sikkim area (2009 – 2015). *Source*: Indian
1329 Meteorological Department (IMD) Gangtok, Sikkim
1330

Year	Jan	Feb	Mar	Apr	May	June	July	Aug	Sep	Oct	Nov	Dec
2009	5.7	4.2	87.3	251.7	335.4	355.4	408.6	454.1	180.1	201.6	1.7	5.4
2010	5.7	18	187	359.4	272.7	504.6	601	493.8	375.8	95.6	23.6	0.1
2011	21.6	40.5	68.5	14.7	278.8	515.9	587.3	459.1	376.7	44.9	60.8	2.3
2012	17.8	21.5	28.4	312.2	201.6	614.4	481.3	442.2	410.9	72.4	0.1	1
2013	4.3	32.1	128	256.1	409	382.6	412.1	325.1	195.5	191.8	40.7	7.9
2014	0	5.4	68.2	96.1	441.4	472.7	478.7	522.3	273	16.7	2.4	4.2
2015	7.4	17.4	73.3	270.3	387.8	603.1	561	284.7	316.1	99.6	55.8	1

1331

1332 Table 5. Spatial relationship between each landslide conditioning factors and observed landslides
1333 Using Frequency Ratio (FR), Information Value (IV) and Certainty Factor (CF) models for all
1334 landslide causative factors classes.

1335

Factors	Class	Class pixel	Landslide pixel	*Npix(Xj)*	*Npix(SXi)*	FR	*Si/Ni*	*S/N*	IV	*PPa*	*PPs*	CF
Elevation (m)	4100 – 3110	6841	218	0.30	0.09	3.42	0.30	0.01	1.51	0.0319	0.0093	0.714
	3110 – 2516	16104	338	0.47	0.21	2.25	0.47	0.01	1.70	0.0210	0.0093	0.561
	2516 – 1993	20031	139	0.19	0.26	0.74	0.19	0.01	1.32	0.0069	0.0093	-0.257
	1993 – 1495	19285	16	0.02	0.25	0.09	0.02	0.01	0.38	0.0008	0.0093	-0.912
	1495 - 816	14545	5	0.01	0.19	0.04	0.01	0.01	-0.13	0.0003	0.0093	-0.963
Geology	gorubathan formation	9312	6	0.01	0.12	0.07	0.01	0.01	-0.05	0.0006	0.0093	-0.931
	lingtse genesis	4112	0	0	0.05	0	0	0.01	0	0.0000	0.0093	-1.000
	basic intrusive	16210	54	0.08	0.21	0.36	0.08	0.01	0.91	0.0033	0.0093	-0.645
	chungthang formation	14123	255	0.36	0.18	1.94	0.36	0.01	1.58	0.0181	0.0093	0.488
	kanchanjangha formation	33049	401	0.56	0.43	1.30	0.56	0.01	1.78	0.0121	0.0093	0.234
Slope (in degree)	70.09 – 45.57	7799	114	0.16	0.10	1.57	0.16	0.01	1.23	0.0146	0.0093	0.366
	45.57 – 35.14	15677	210	0.29	0.20	1.44	0.29	0.01	1.50	0.0134	0.0093	0.307
	35.14 – 25.53	20253	218	0.30	0.26	1.15	0.30	0.01	1.51	0.0108	0.0093	0.135
	25.53 – 15.37	20229	126	0.18	0.26	0.67	0.18	0.01	1.28	0.0062	0.0093	-0.334
	15.37 - 0	12848	48	0.07	0.17	0.40	0.07	0.01	0.86	0.0037	0.0093	-0.601
Soil	fine skeletal	5224	1	0.00	0.07	0.02	0.00	0.01	-0.82	0.0002	0.0093	-0.980

	coarse loamy distrudeptic	32878	127	0.18	0.43	0.41	0.18	0.01	1.28	0.0039	0.0093	-0.588
	coarse loamy holithic	11997	156	0.22	0.16	1.39	0.22	0.01	1.37	0.0130	0.0093	0.286
	fine loamy	6534	0	0	0.09	0	0	0.01	0	0.0000	0.0093	-1
	loamy skeletal	3754	126	0.18	0.05	3.60	0.18	0.01	1.28	0.0336	0.0093	0.729
	coarce loamy	16419	306	0.43	0.21	2.00	0.43	0.01	1.66	0.0186	0.0093	0.505
Drainage Density	9.55 – 6.25	12033	62	0.09	0.16	0.55	0.09	0.01	0.97	0.0052	0.0093	-0.450
	6.25 – 4.92	18190	73	0.10	0.24	0.43	0.10	0.01	1.04	0.0040	0.0093	-0.572
	4.92 – 3.62	17869	140	0.20	0.23	0.84	0.20	0.01	1.32	0.0078	0.0093	-0.161
	3.62 – 2.17	16626	312	0.44	0.22	2.01	0.44	0.01	1.67	0.0188	0.0093	0.508
	2.17 – 0.09	12088	129	0.18	0.16	1.14	0.18	0.01	1.29	0.0107	0.0093	0.128
Road Density	11.17 – 6.86	2051	13	0.02	0.03	0.68	0.02	0.01	0.29	0.0063	0.0093	-0.322
	6.86 – 4.48	4530	100	0.14	0.06	2.37	0.14	0.01	1.18	0.0221	0.0093	0.583
	4.48 – 2.55	8439	252	0.35	0.11	3.20	0.35	0.01	1.58	0.0299	0.0093	0.694
	2.55 – 0.88	14317	157	0.22	0.19	1.18	0.22	0.01	1.37	0.0110	0.0093	0.151
	0.88 – 0	47469	194	0.27	0.62	0.44	0.27	0.01	1.46	0.0041	0.0093	-0.564
Rainfall (mm)	1847 – 2386	6624	263	0.37	0.09	4.26	0.37	0.01	1.60	0.0397	0.0093	0.758
	2386 – 2791	5199	95	0.13	0.07	1.96	0.13	0.01	1.15	0.0183	0.0093	0.485
	2791 – 3096	12076	137	0.19	0.16	1.22	0.19	0.01	1.31	0.0113	0.0093	0.177
	3096 – 3323	31797	195	0.27	0.41	0.66	0.27	0.01	1.47	0.0061	0.0093	-0.515
	3323 – 3657	21110	26	0.04	0.27	0.13	0.04	0.01	0.59	0.0012	0.0093	-6.508
NDVI	0.64 – 0.43	9717	205	0.29	0.13	2.26	0.29	0.01	1.49	0.0211	0.0093	0.563
	0.43 – 0.34	13283	160	0.22	0.17	1.29	0.22	0.01	1.38	0.0120	0.0093	0.228
	0.34 – 0.24	17463	90	0.13	0.23	0.55	0.13	0.01	1.13	0.0052	0.0093	-0.816
	0.24 – 0.14	21584	92	0.13	0.28	0.46	0.13	0.01	1.14	0.0043	0.0093	-1.198
	0.14 - -0.11	14759	169	0.24	0.19	1.23	0.24	0.01	1.40	0.0115	0.0093	0.188
Curvature	CONCAVE	43887	375	0.52	0.57	0.92	0.52	0.01	1.75	0.0085	0.0093	-0.084
	FLAT	14592	90	0.13	0.19	0.66	0.13	0.01	1.13	0.0062	0.0093	-0.516
	CONVEX	18327	251	0.35	0.24	1.47	0.35	0.01	1.58	0.0137	0.0093	0.322
TPI	15.25 – 11.26	6669	67	0.09	0.09	1.08	0.09	0.01	1.00	0.0100	0.0093	0.073
	11.26 – 10.15	18765	173	0.24	0.24	0.99	0.24	0.01	1.41	0.0092	0.0093	-0.011
	10.15 – 9.19	25823	228	0.32	0.34	0.95	0.32	0.01	1.53	0.0088	0.0093	-0.053
	9.19 – 8.31	18956	171	0.24	0.25	0.97	0.24	0.01	1.41	0.0090	0.0093	-0.033
	8.31 – 5.83	6593	77	0.11	0.09	1.25	0.11	0.01	1.06	0.0117	0.0093	0.204
SPI	145.4 – 47.88	133	0	0	0.002	0	0	0.01	0	0	0.0093	-1
	47.88 – 20.52	1060	7	0.01	0.01	0.71	0.01	0.01	0.02	0.0066	0.0093	-0.294
	20.52 – 9.12	4966	57	0.08	0.06	1.23	0.08	0.01	0.93	0.0115	0.0093	0.190
	9.12 – 2.85	21030	255	0.36	0.27	1.30	0.36	0.01	1.58	0.0121	0.0093	0.233
	2.85 – 0	49617	397	0.55	0.65	0.86	0.55	0.01	1.77	0.0080	0.0093	-0.143
TWI	65.13 – 15.18	5334	20	0.03	0.07	0.40	0.03	0.01	0.48	0.0037	0.0093	-0.600
	15.18 – 4.59	13142	65	0.09	0.17	0.53	0.09	0.01	0.99	0.0049	0.0093	-0.472
	4.59 - - 4.48	21264	206	0.29	0.28	1.04	0.29	0.01	1.49	0.0097	0.0093	0.038
	-4.5 - - 14.57	22952	263	0.37	0.30	1.23	0.37	0.01	1.60	0.0115	0.0093	0.188
	-14.6 - - 63.5	14114	162	0.23	0.18	1.23	0.23	0.01	1.39	0.0115	0.0093	0.190

LULC	Step cultivation	1648	0	0	0.02	0	0	0.01	0	0	0.0093	-1
	dense forest	45962	309	0.43	0.60	0.72	0.43	0.01	1.67	0.0067	0.0093	-0.281
	settlement	3865	7	0.01	0.05	0.19	0.01	0.01	0.02	0.0018	0.0093	-0.807
	bare soil	3921	149	0.21	0.05	4.08	0.21	0.01	1.35	0.0380	0.0093	0.762
	river	1439	0	0	0.02	0	0	0.01	0	0	0.0093	-1
	open forest	19971	251	0.35	0.26	1.35	0.35	0.01	1.58	0.0126	0.0093	0.261

Table 6. Multicollinearity analysis of FR, IV and CF approach.

Variable	FR		IV		CF	
	TOL	VIF	TOL	VIF	TOL	VIF
TPI	0.29	3.42	0.30	3.39	0.315	3.177
NDVI	0.53	1.88	0.51	1.98	0.536	1.865
SPI	0.69	1.45	0.69	1.45	0.818	1.222
WI	0.52	1.92	0.52	1.92	0.675	1.481
slope	0.59	1.69	0.59	1.70	0.573	1.744
RD	0.90	1.11	0.86	1.16	0.902	1.109
Curvature	0.38	2.66	0.37	2.67	0.376	2.658
DD	0.50	1.99	0.59	1.69	0.509	1.963
Lulc Class	0.87	1.15	0.87	1.15	0.857	1.166
Geology	0.38	2.63	0.39	2.58	0.38	2.628
Soil	0.65	1.54	0.56	1.78	0.656	1.524
Rainfall	0.25	4.02	0.39	2.57	0.249	4.023
Elevation	0.20	4.96	0.33	3.00	0.176	5.677

1349 Table 7. The comparison between observed landslide and landslide susceptibility model with the
1350 landslide density (LD).

Model	Susceptibility Zones	No. of pixel	Area(Sq.km)	Area (%)	No. of landslide pixel	Area (Sq.km)	Area (%)	Landslide Density
FR_M	Very low	14615	13.15	19.02	3	0.0027	0.42	0.0002
	Low	25282	22.75	32.91	45	0.0405	6.28	0.00178
	Moderate	19438	17.49	25.30	118	0.1062	16.48	0.00607
	High	12783	11.50	16.64	334	0.3006	46.64	0.02612
	Very high	4688	4.21	6.10	216	0.1944	30.16	0.04607
IV_M	Very low	10306	9.27	13.42	0	0	0	0
	Low	16678	15.01	21.71	16	0.14	2.24	0.00096
	Moderate	14742	13.26	19.19	91	0.082	12.71	0.0061
	High	26396	23.75	34.36	423	0.38	59.07	0.016
	Very high	8684	7.81	11.31	186	0.167	25.98	0.021
CF_M	Very low	15337	13.80	19.97	3	0.003	0.42	0.0002
	Low	25564	23.01	33.28	47	0.042	6.6	0.0018
	Moderate	11509	10.35	14.98	57	0.051	7.9	0.005
	High	12740	11.46	16.59	139	0.125	19.41	0.0109
	Very high	11656	10.49	15.18	470	0.423	65.68	0.0403

1351

1352 Table 8. The overall statistics in the various model of the ROC curve.

Test result models	Area under curve	Standard error	Asymptotic significance	Asymptotic 99 % confidence level	
				Lower bound	Upper bound
FR model	0.828	0.016	0.000	0.788	0.868
IV model	0.836	0.015	0.000	0.797	0.875
CF model	0.750	0.019	0.000	0.701	0.799

1353

Figures

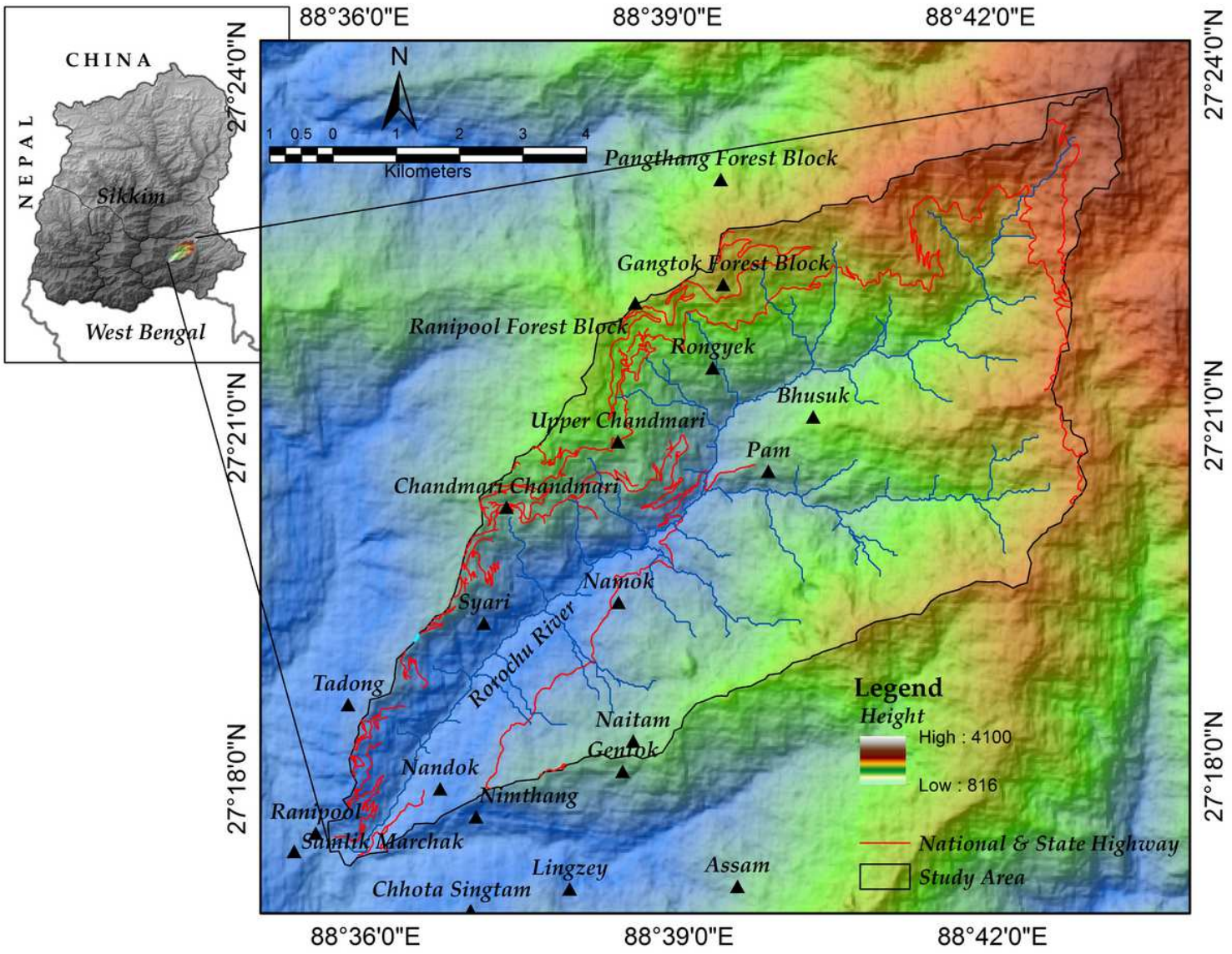

Figure 1

Location map of the study area

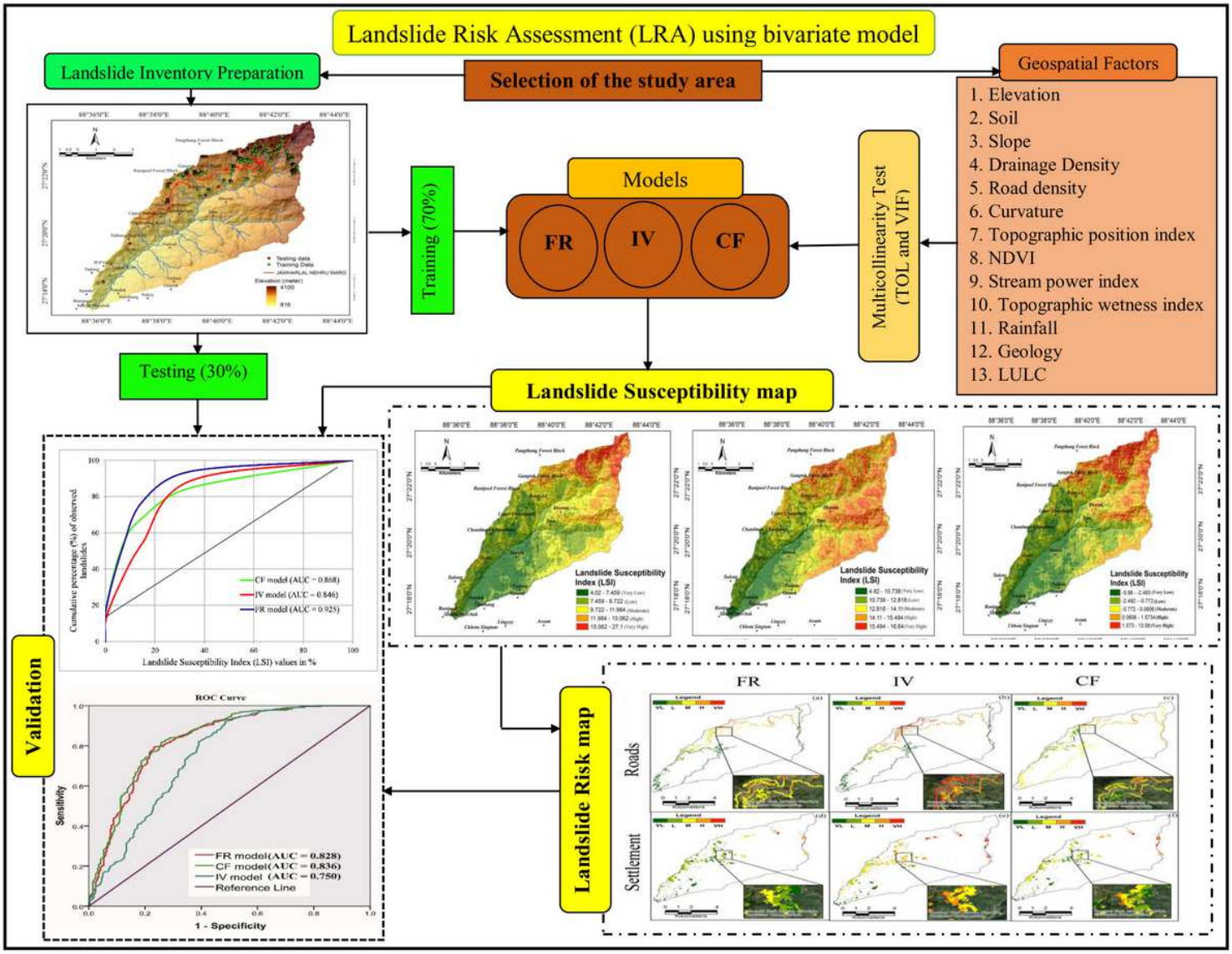

Figure 2

Methodological flow chart

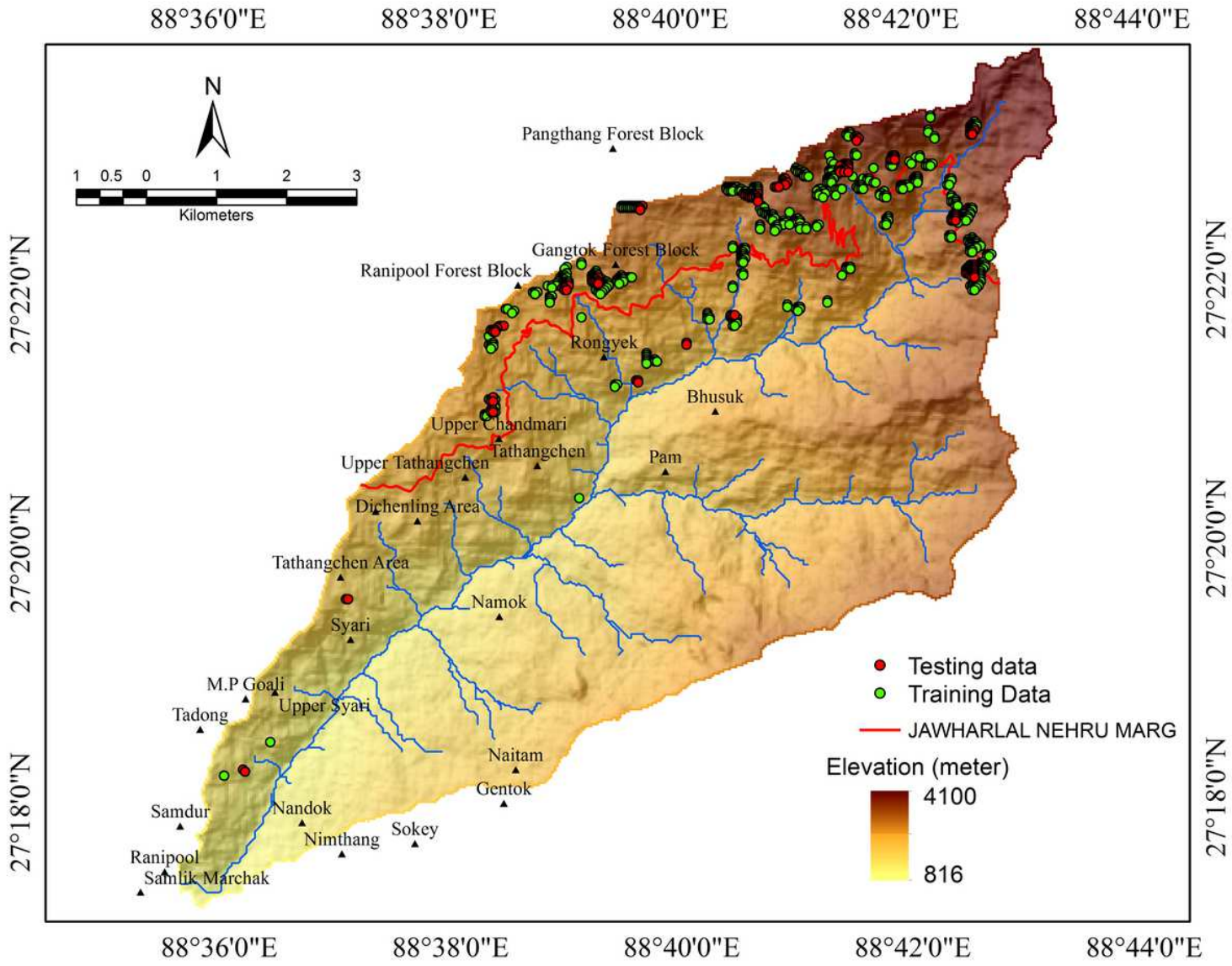

Figure 3

Landslide inventory map of Rorachu watershed

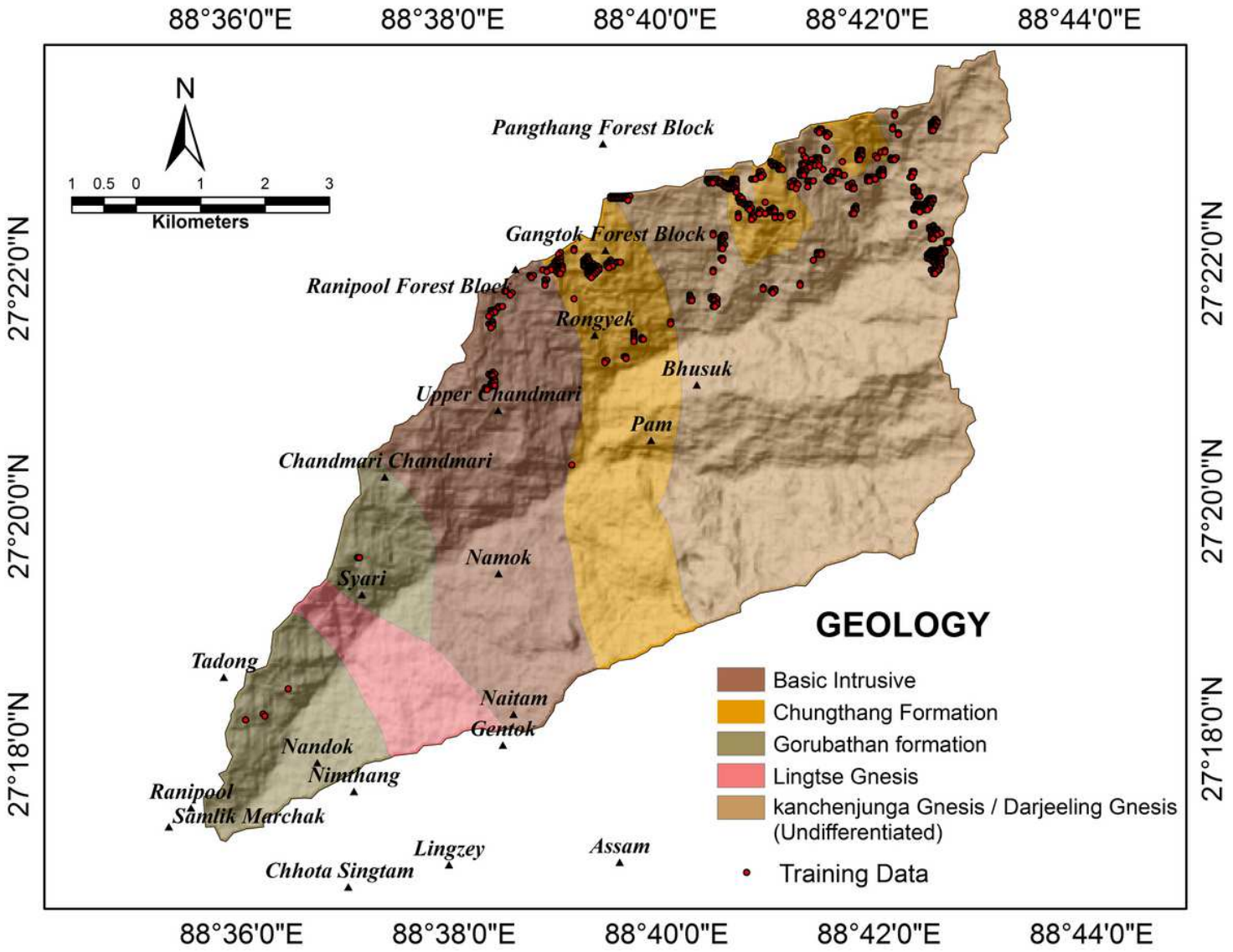

Figure 4

Geological map of the study area

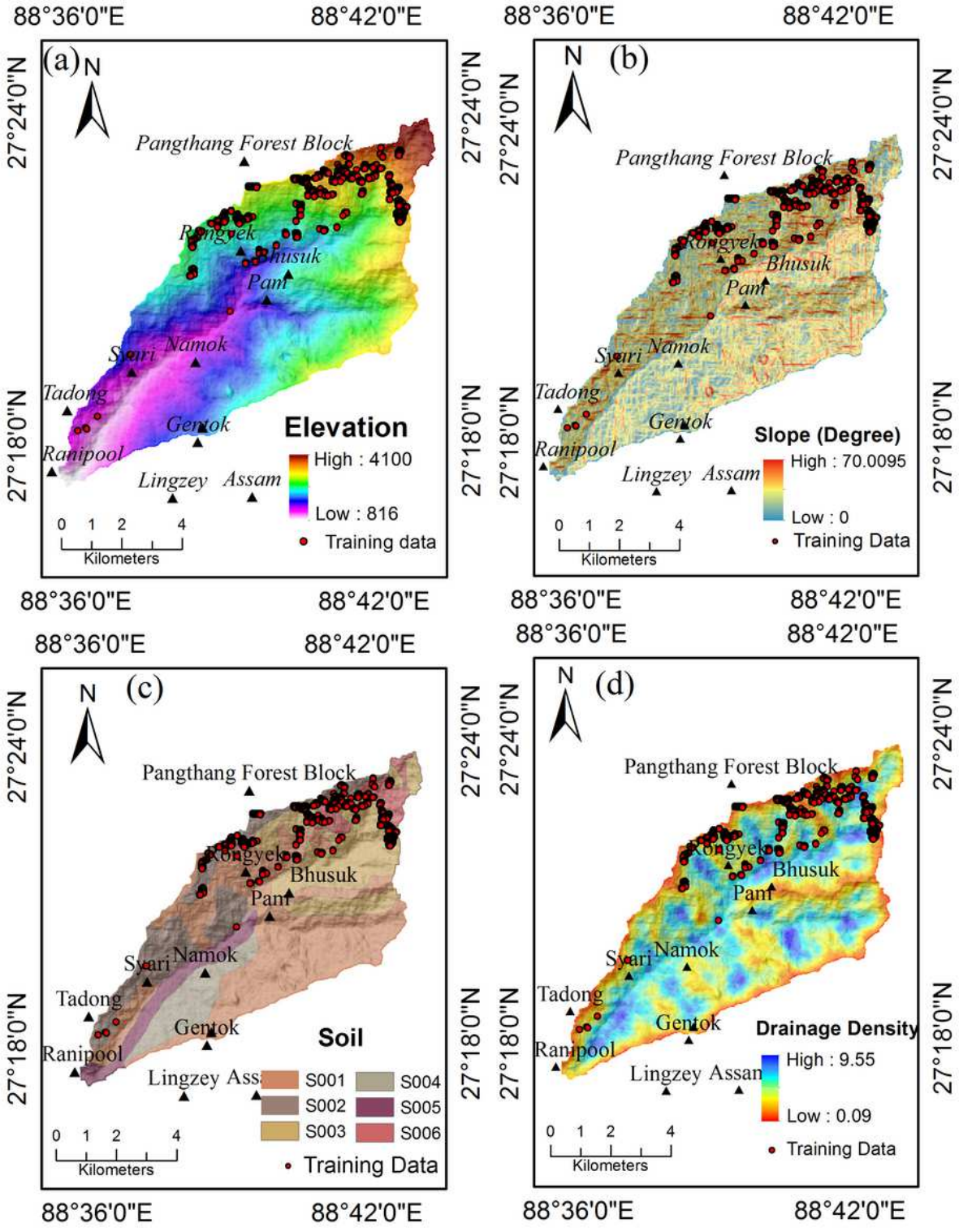

Figure 5

Landslide conditioning factors a. Elevation b. Slope c. Soil d. Drainage density

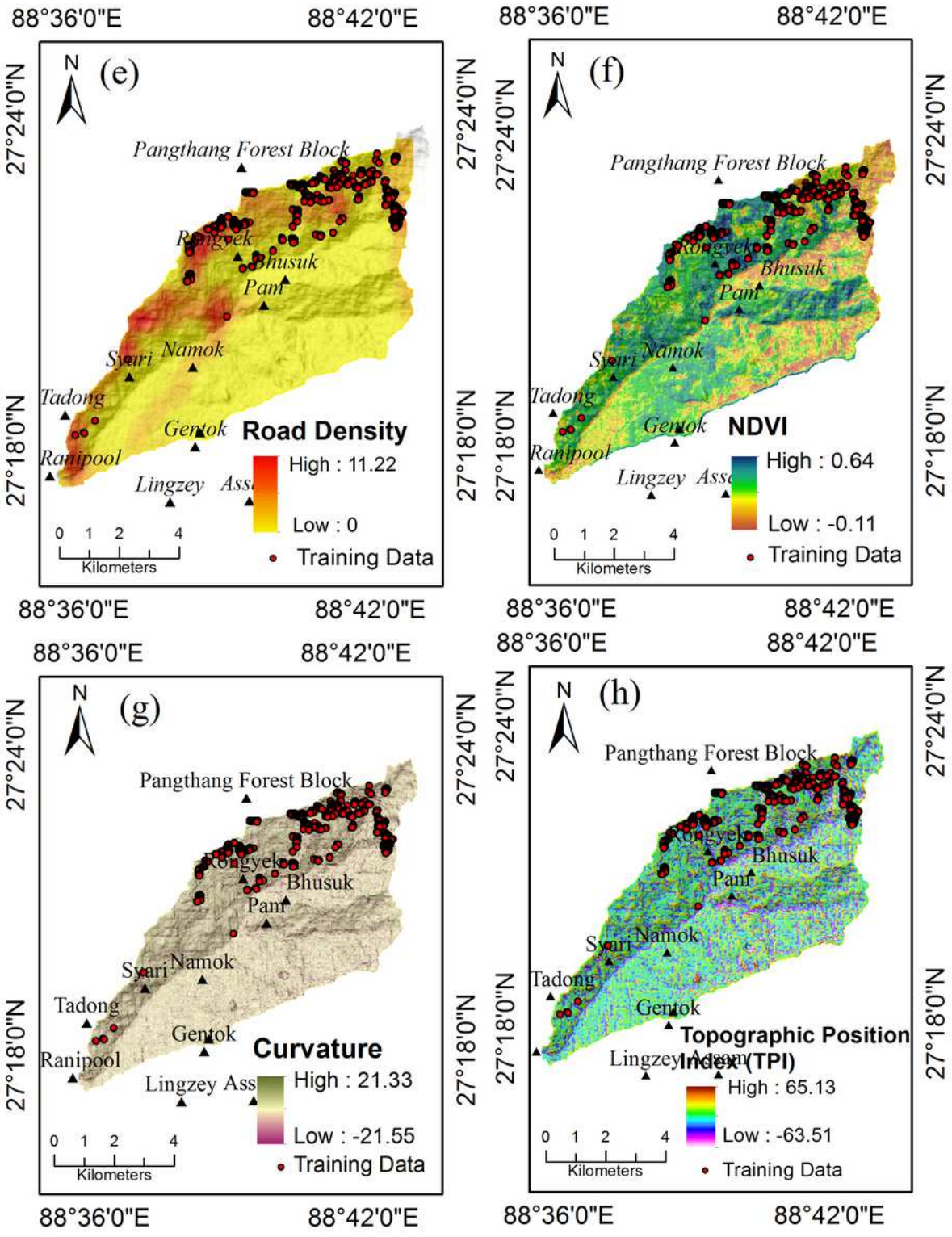

Figure 6

Landslide conditioning factors e. Road density f. NDVI g. Aspect h. Topographic position index (TPI)

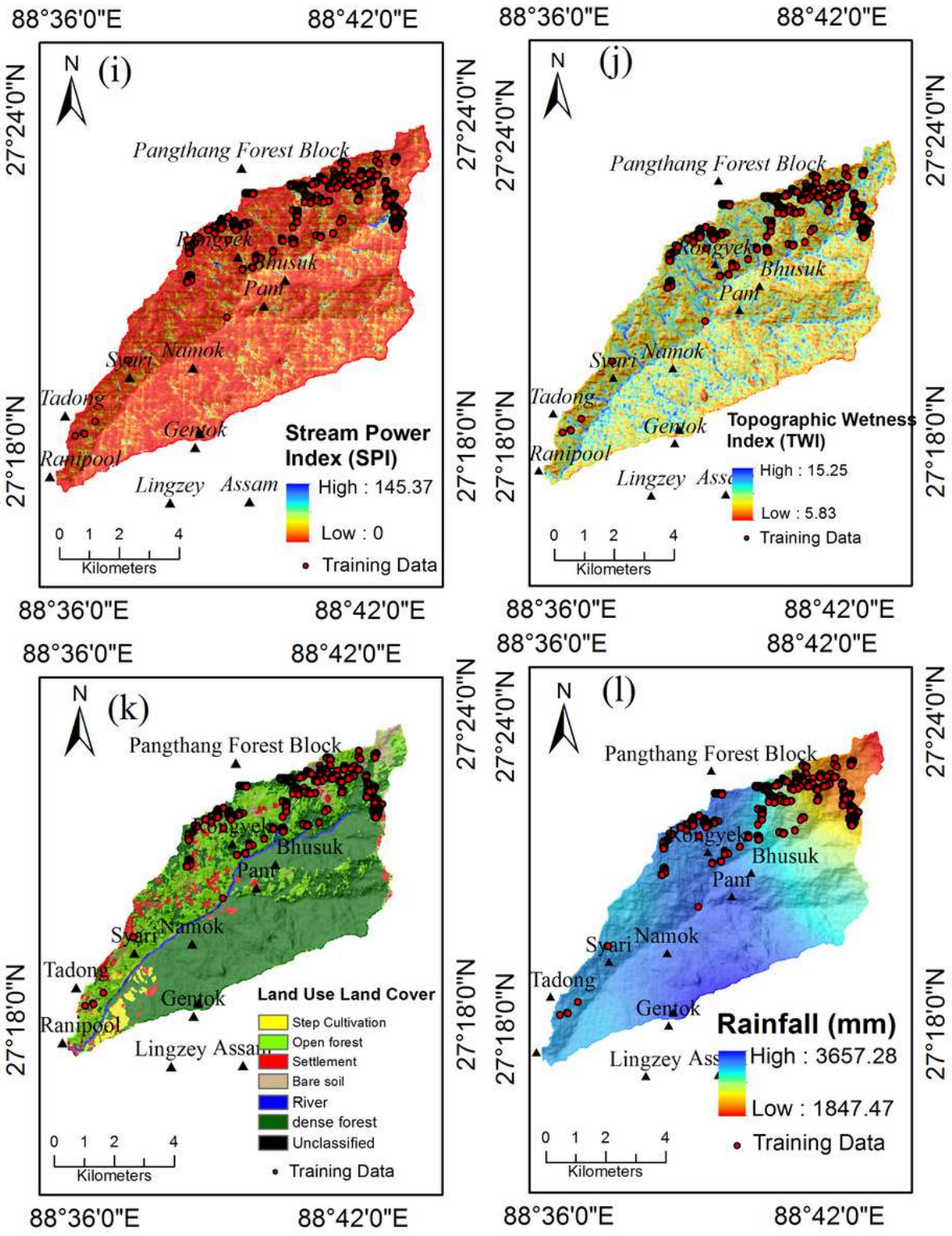

Figure 7

Landslide conditioning factors i. Stream power index (SPI) j. Topographic position index (TPI) k. Land use land cover (LULC) l. Rainfall

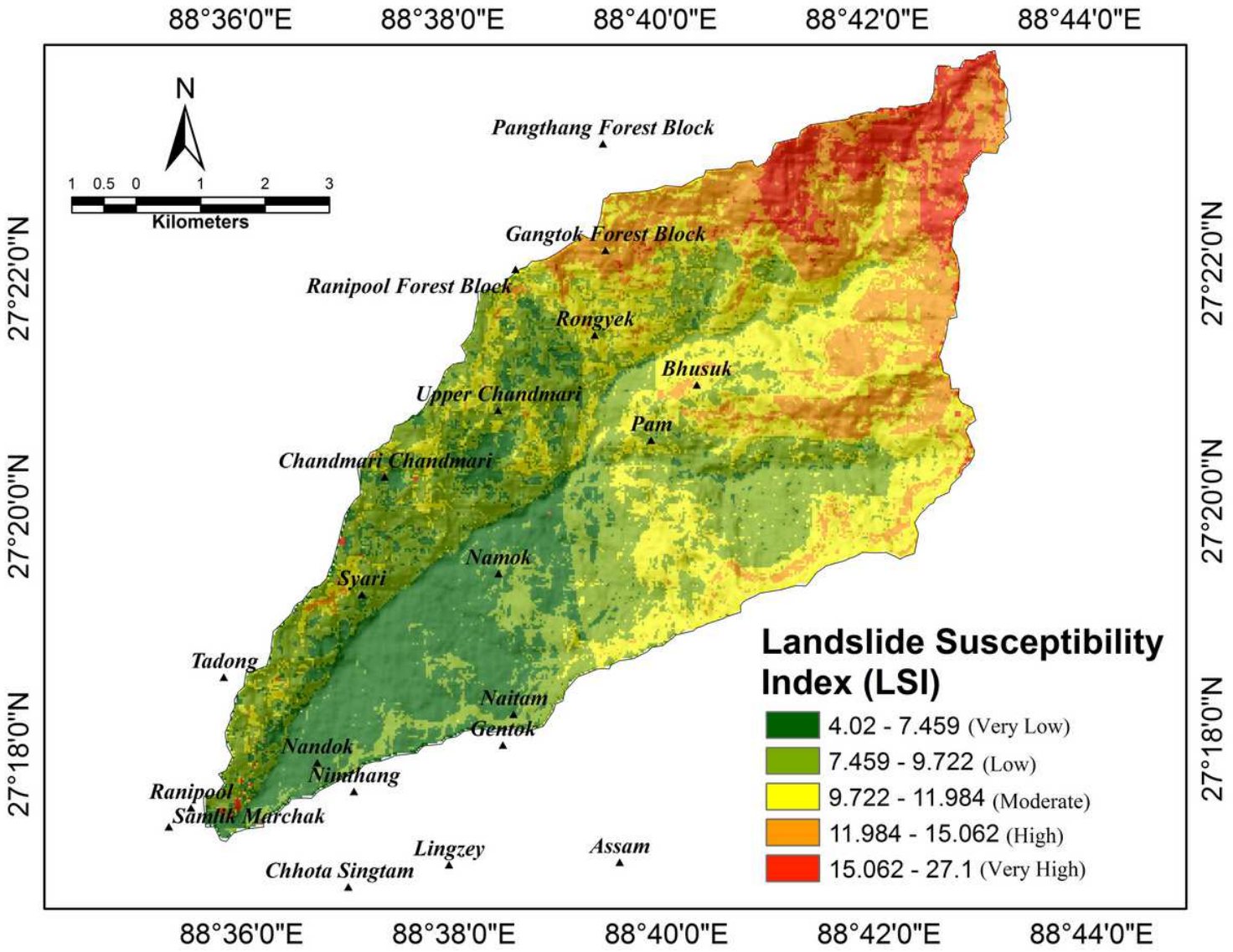

Figure 8

Landslide susceptibility map emanated by Frequency Ratio (FR) model

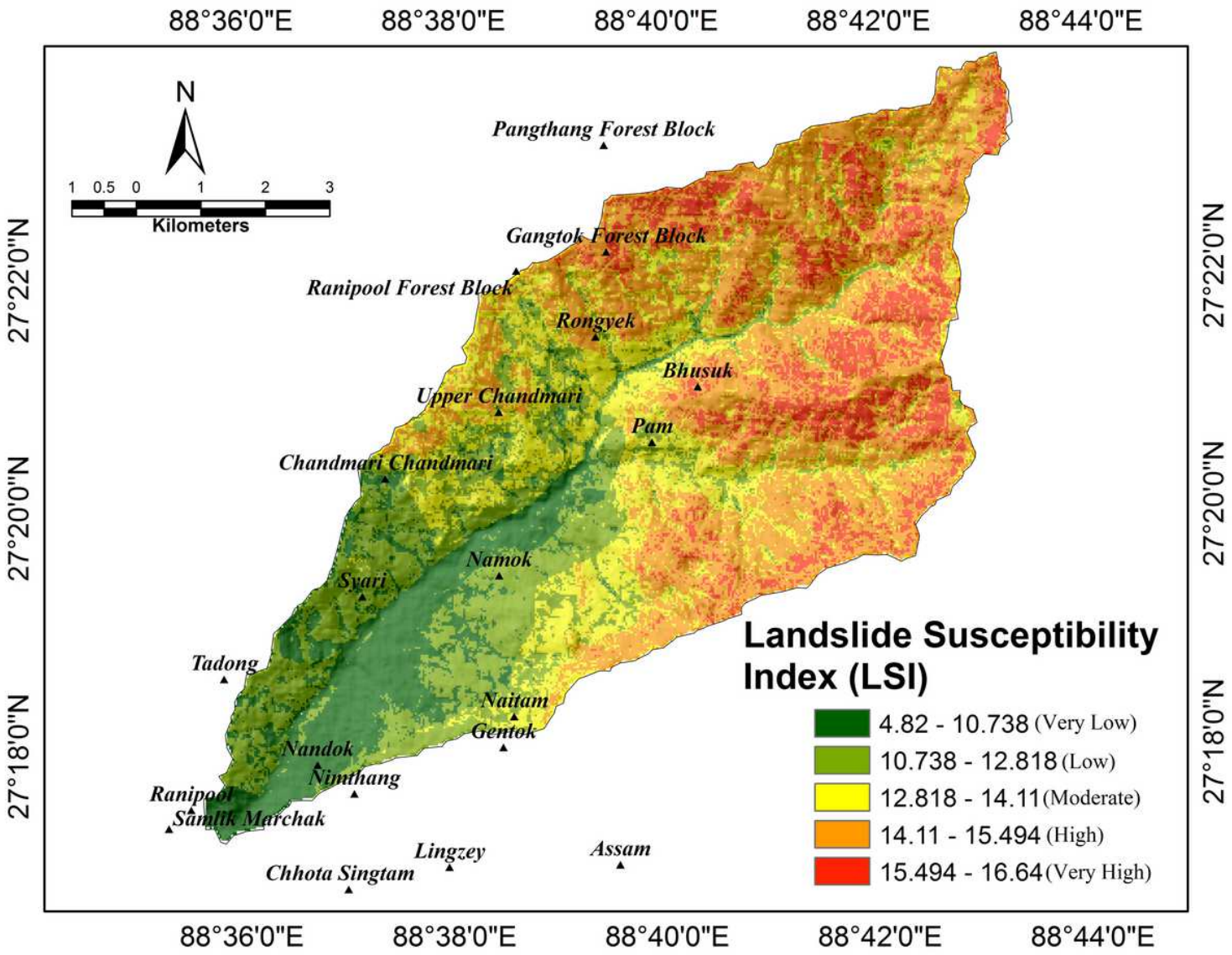

Figure 9

Landslide susceptibility map emanated by Information Value (IV) model

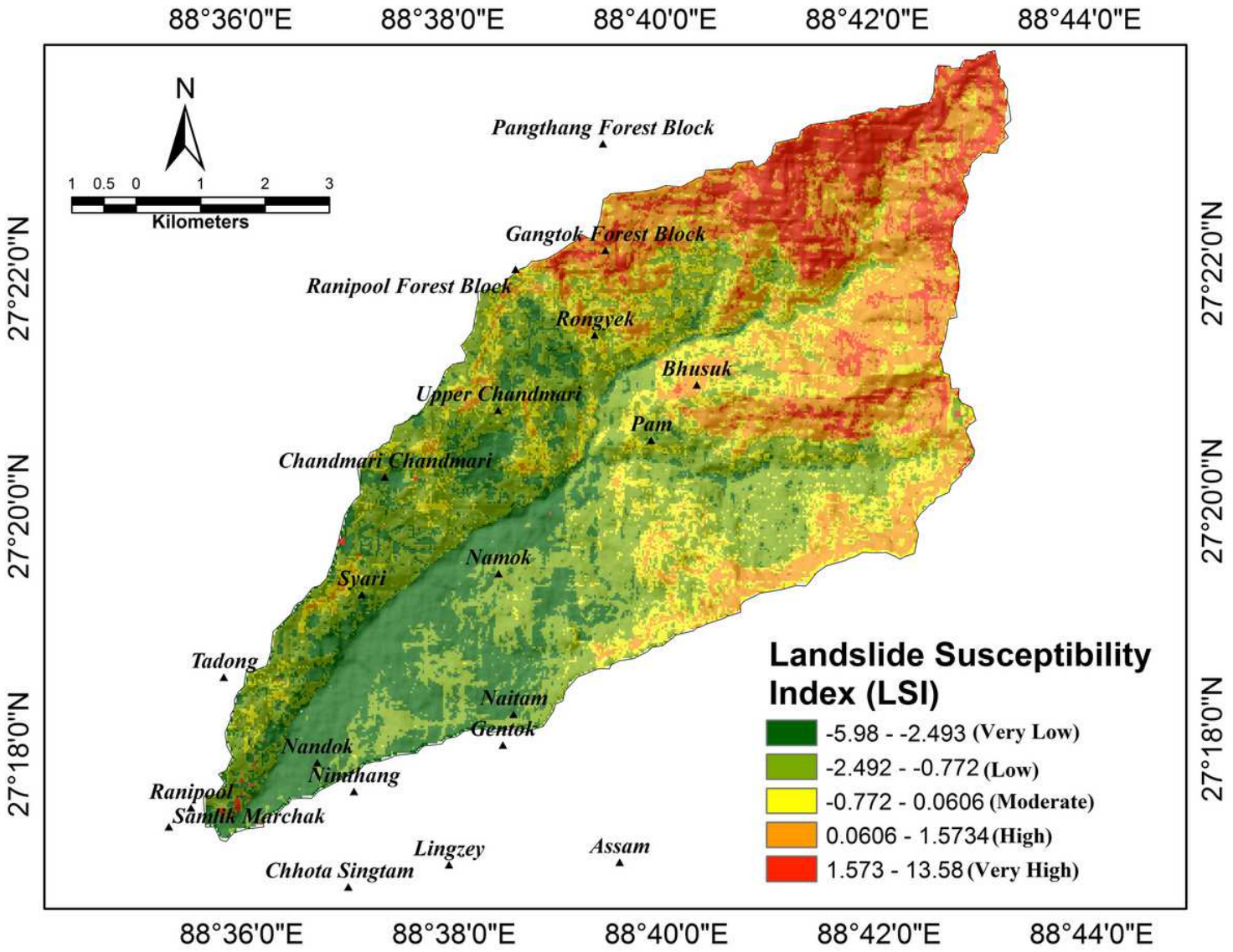

Figure 10

Landslide susceptibility map emanated by Certainty Factor (CF) model

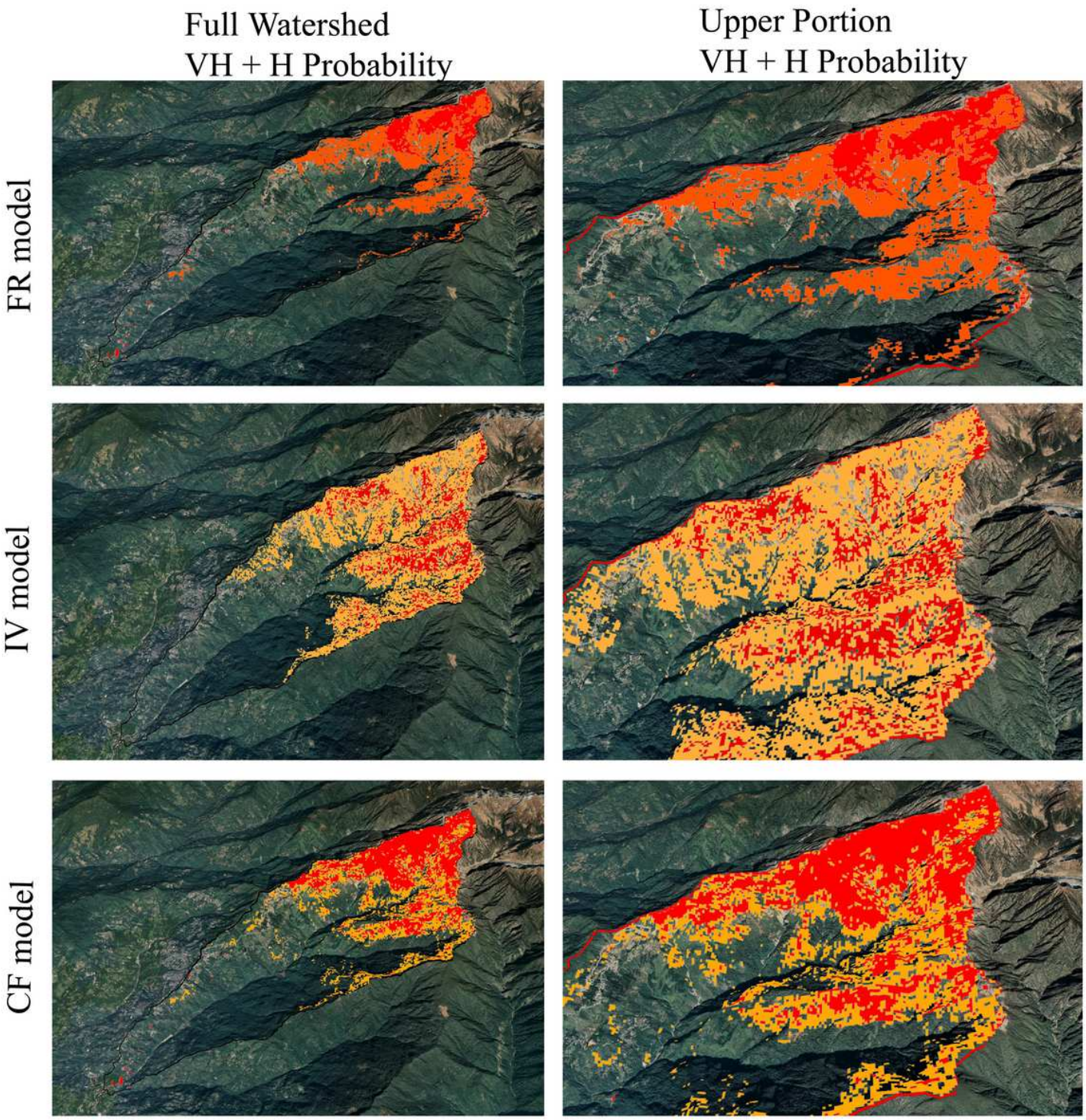

Figure 11

Google earth map showing the very high (VH) and high (H) landslide susceptibility of various models (FR, IV and CF).

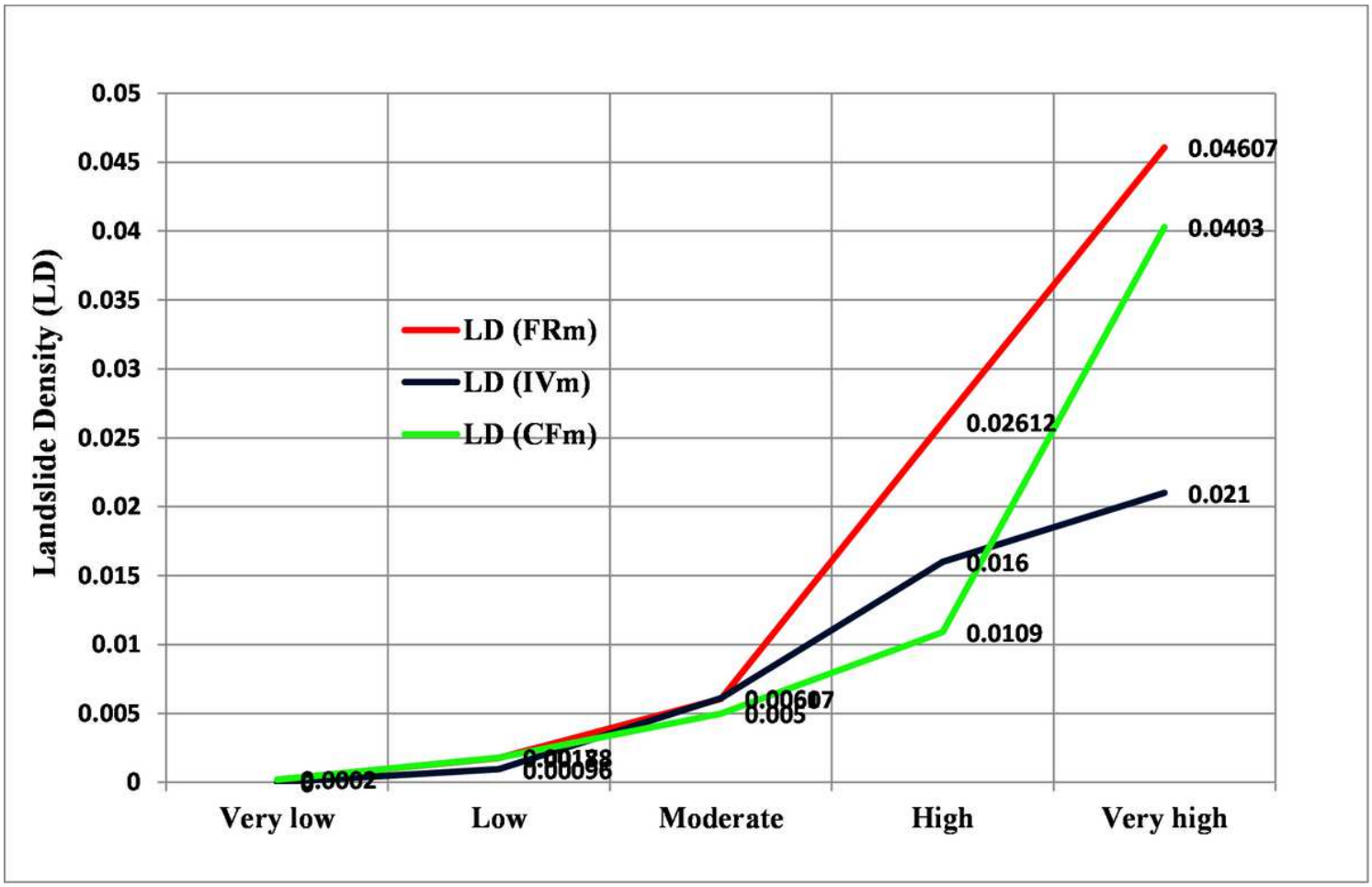

Figure 12

The landslide density (LD) has been showing the increasing trend to the highest vulnerable areas.

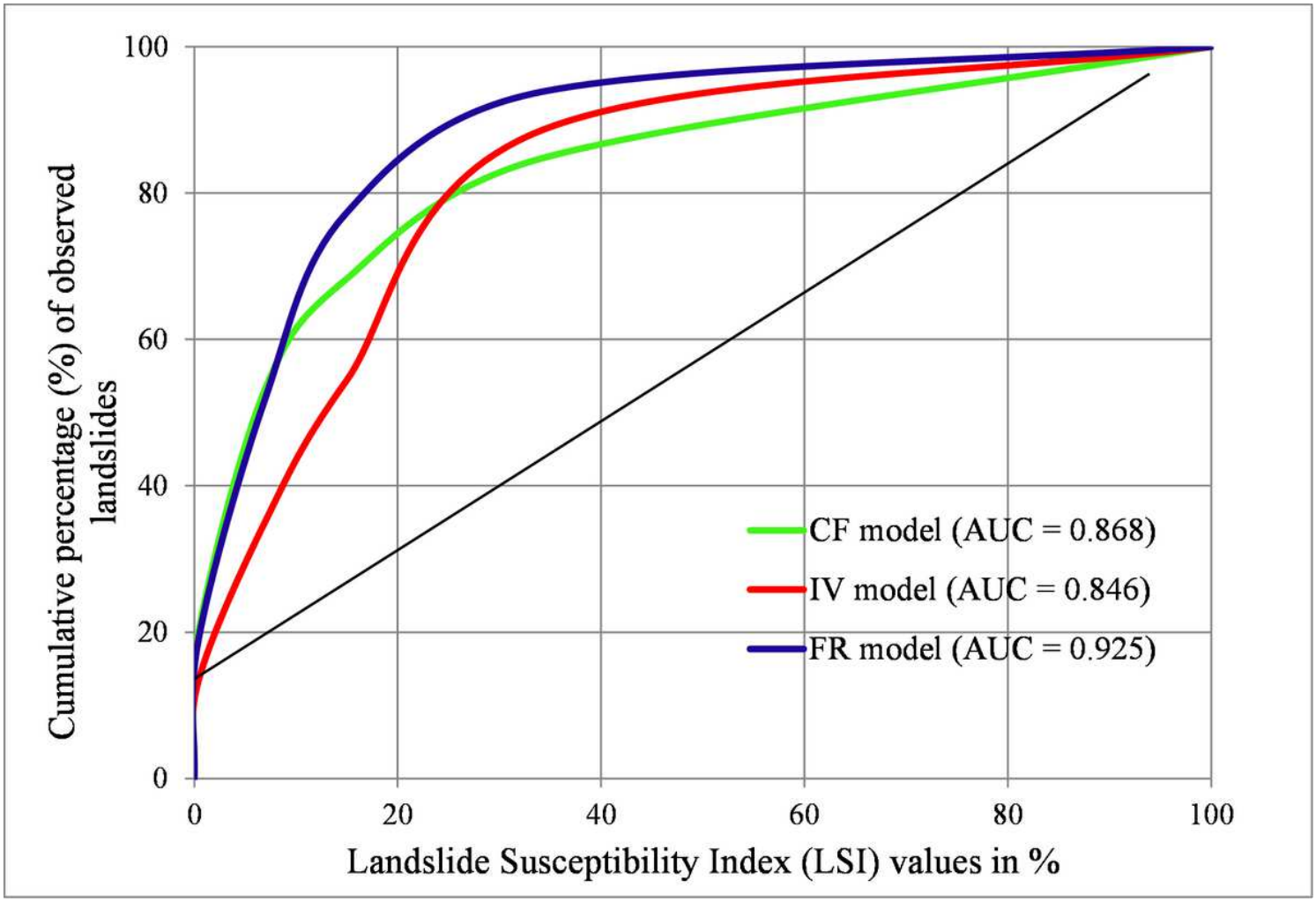

Figure 13

Success rate curve (SRC) for the three models (FR, IV and CF) in the Rorachu watershed

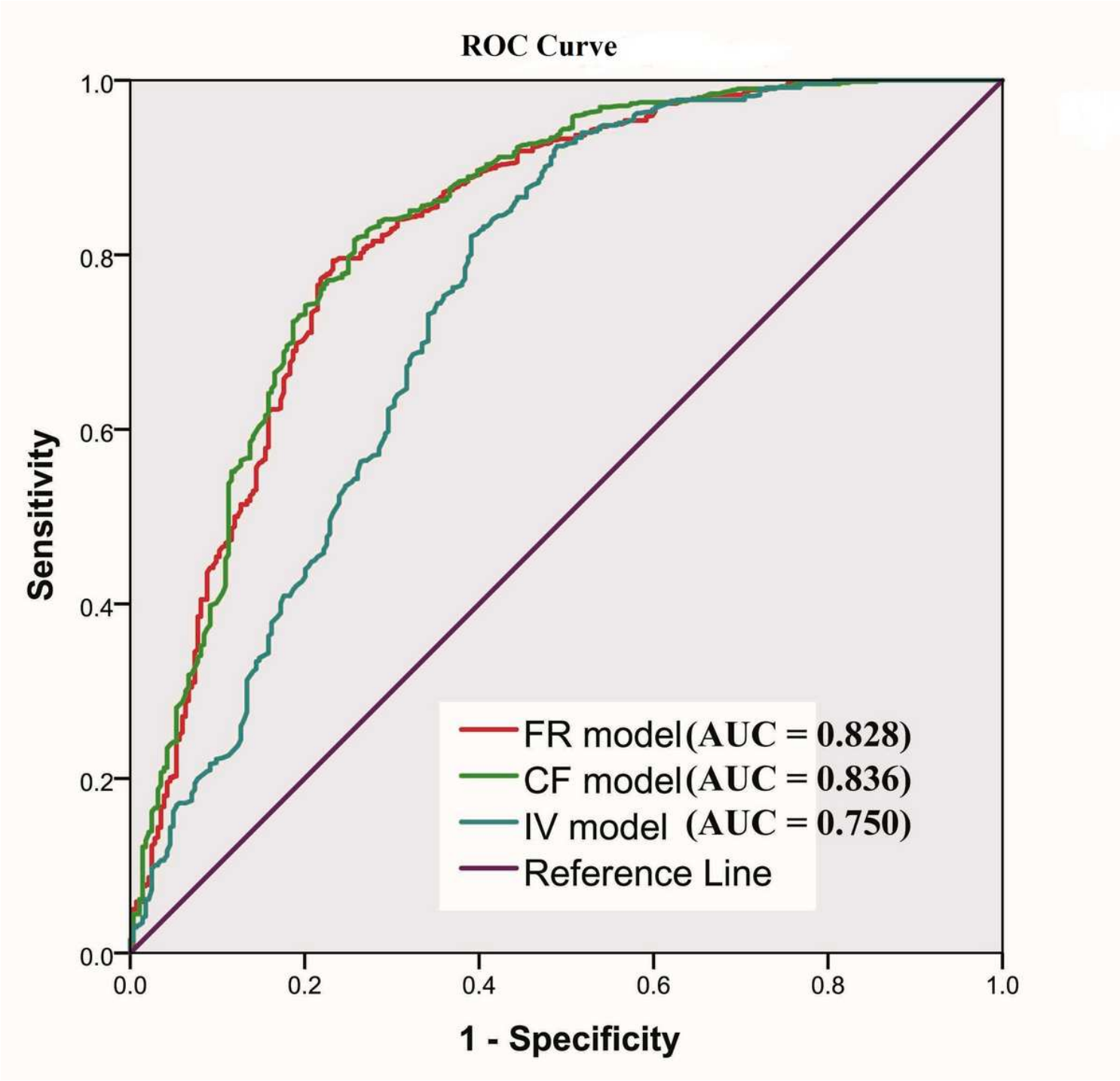

Figure 14

Receive operating characteristics (ROC) curve for the FR, IV and CF models.

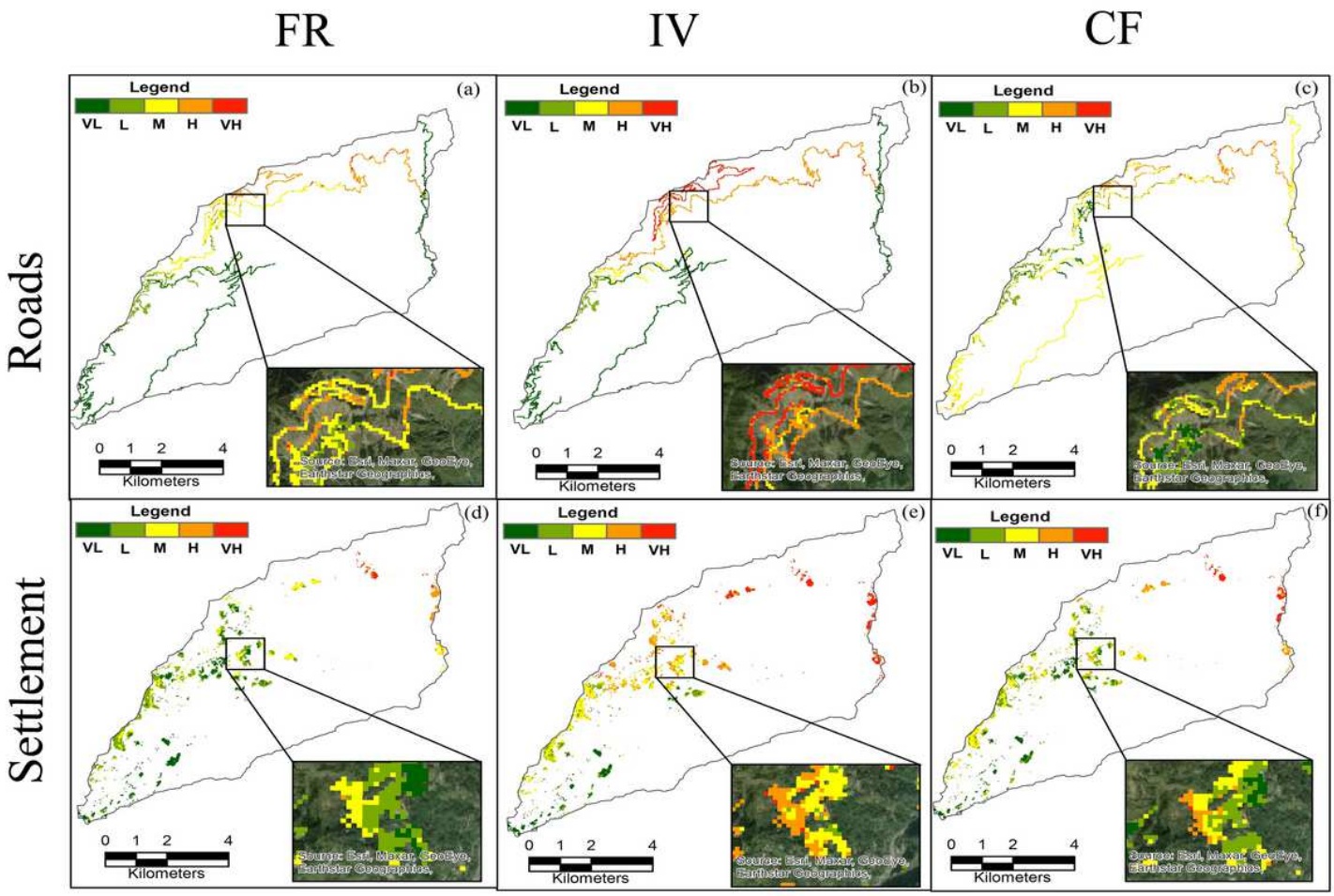

Figure 15

Landslide risk map of two variables (Settlement and Road) by the various models (a) Road risk map by Frequency Ratio (FR) model, (b) Road risk map by Information Value (IV) model, (c) Road risk map by Certainty Factor (CF) model, (d) Settlement risk map by Frequency Ratio (FR) model, (e) Settlement risk map by Information Value (IV) model and (f) Settlement risk map by Certainty Factor (CF) model

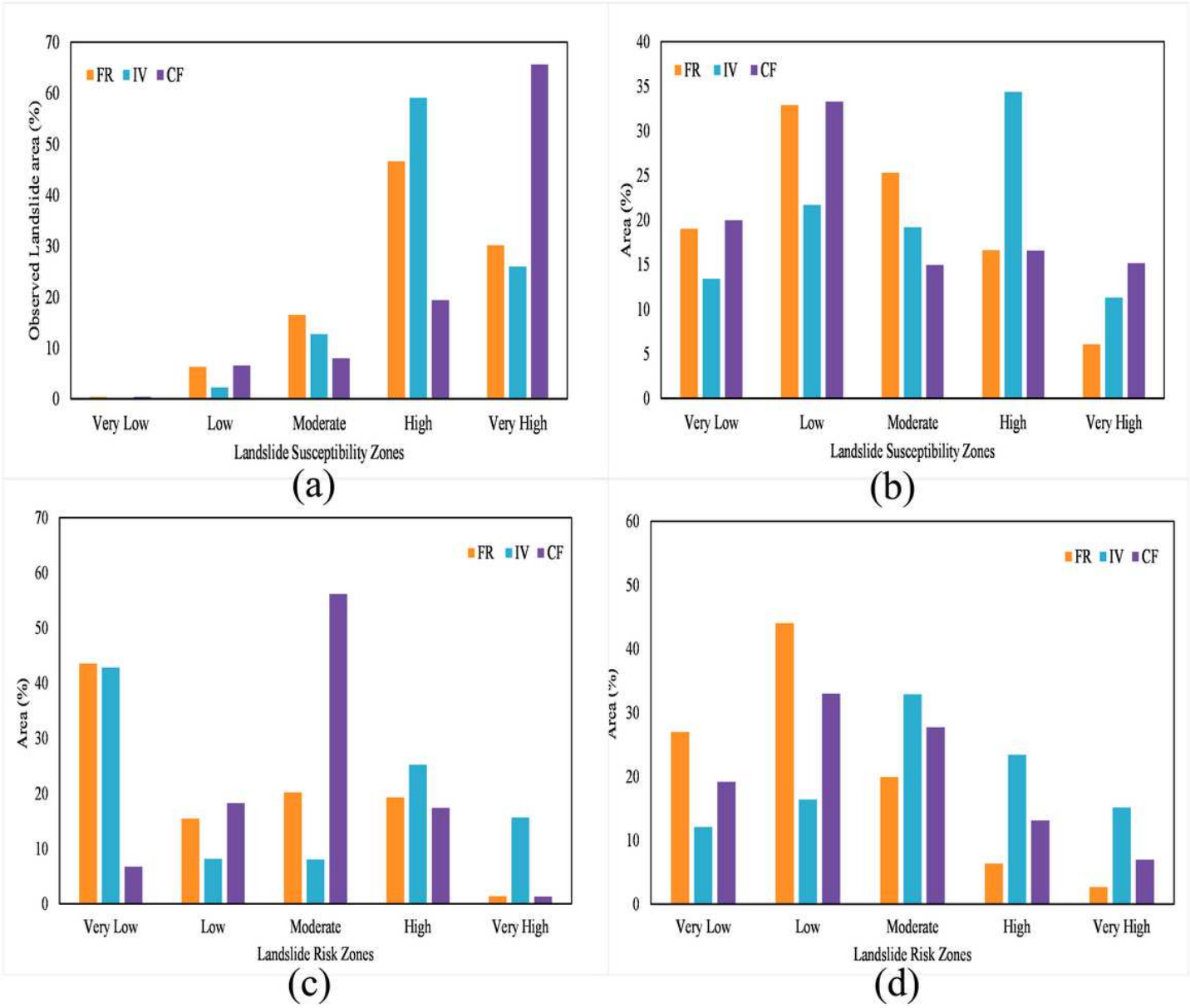

Figure 16

The comparative Bar graph revealing the areal distribution of numerous models (FR, IV and CF) a. observed landslide area situated in various landslide susceptibility zones b. Areal distribution of landslide susceptibility zones c. Areal distribution of Roads in various landslide risk zones (LRZ) d. Areal distribution of Settlement in various landslide risk zones (LRZ).

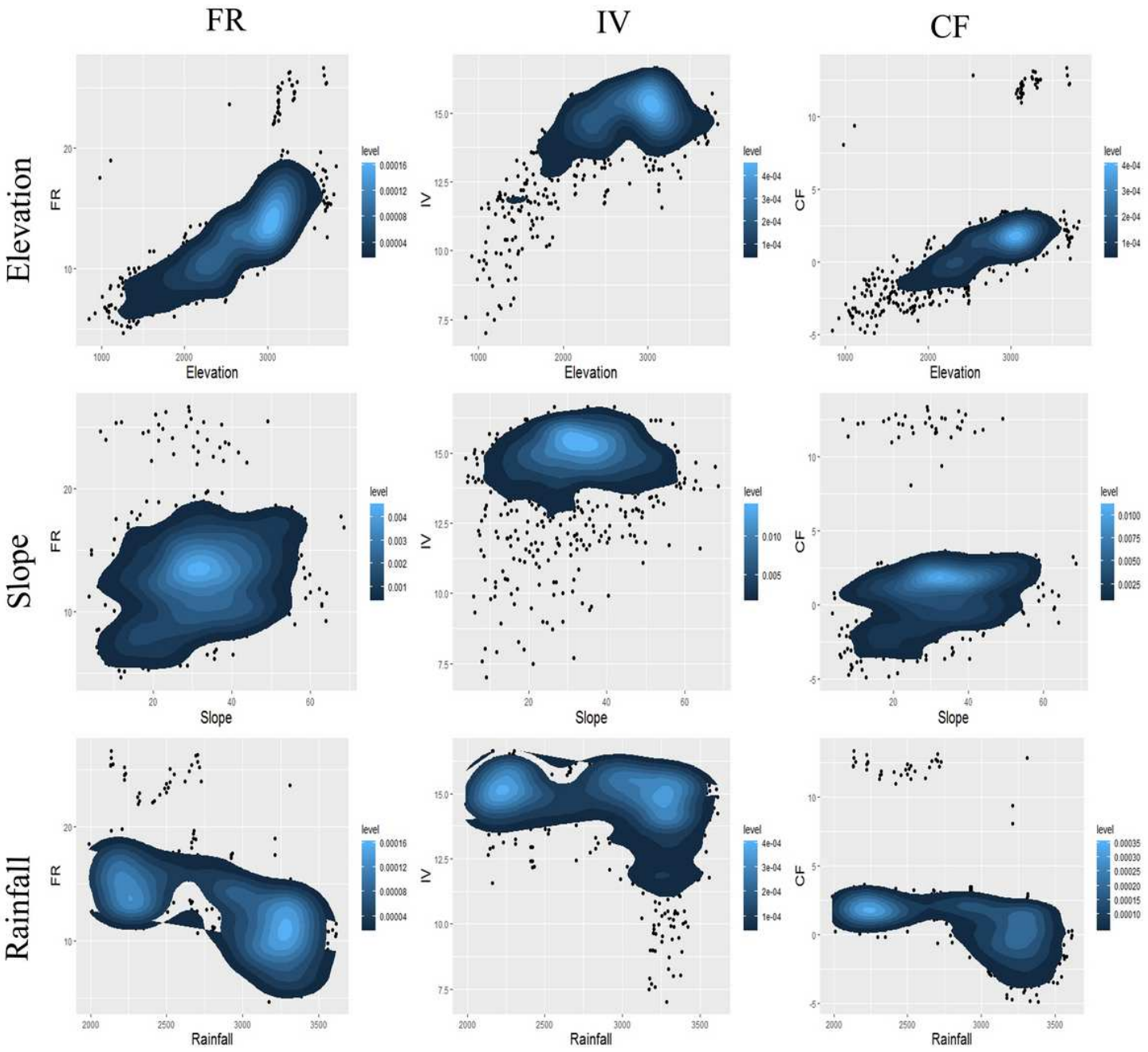

Figure 17

The probability of landslide vulnerability in various ranges (Elevation, Slope and Rainfall).